Dear Editor,
thank you for your additional feedback regarding our manuscript. We can address the remaining two questions as follows:

Question #1:
Labile C: I remain confused by your added text on this matter. Is allocation to labile capped at 40% (i.e. a flux cap), or is the labile pool total capped at 40% of another pool's value (i.e. a stock cap)? Perhaps an equation would clarify. What happens once the cap is reached in terms of using the C that would have been allocated to labile? Is GPP down regulated, or is there excess respiration?

The 40% allocated to the labile stem pool is not a cap (or maximum value), but rather a constant fraction in the allocation (flux). The remaining C is allocated to the non-labile stem pool. Because the labile stem pool can be relocated, it can reach a maximum value of 40% of the total C in stems, but will in practice be below that. Since we use a fixed fraction of the daily photosynthetic carbon gain there is therefore no need to downregulate GPP or upregulate respiration. The reviewer is correct that this was a bit tricky to understand, hoping to clarify this to the reader, we revised the following sentence:

"To represent this in the model, a labile C pool is filled with a fraction of the C allocated to the stem, set here to 0.4 for wheat (Penning de Vries et al., 1989), and thus has a cap of the allocation to stem ($g_{St}$) times 0.4."

to read as follows in the current version of the manuscript:

"To represent this in the model, a labile C pool is filled with a fraction of the daily assimilates directed to the stem ($g_{St}$), set here to 0.4 for wheat (Penning de Vries et al., 1989). The labile C pool ($M_{\mathrm{C,labile}}$) is constrained between 0 and $0.4M_{\mathrm{C,St}}$."
(page 11 line 3)

Question #2:
For labile N it is not clear how this pool is constrained by leave and roots N sources. Do you mean sinks?

Leaves and roots are normally sinks for N indeed, but can be sources for N to the labile pool when translocation occurs. In this case, the labile pool is really a short-term storage for senesced N waiting to be transported to the storage organs. We mention this in the revised text to make it more clear. We revised the following:

"In contrast to the labile C pool, there is no explicit cap on this pool, but the amount is constrained since leaves and roots act as labile N sources."

to read as follows:

"In contrast to the labile C pool, N allocated to the labile pool is not determined as a fraction of the total allocation. The amount is constrained by the N translocated from senesced leaves (Eq. 14) and roots accordingly through the functional balance concept (Eq. 10)."
(page 14 line 13)

with best regards,
Stefan Olin on behalf of all authors

Manuscript prepared for Biogeosciences Discuss.
with version 2014/07/29 7.12 Copernicus papers of the LaTeX class copernicus.cls.
Date: 10 April 2015

# Modelling the response of yields and tissue C : N to changes in atmospheric $CO_2$ and N management in the main wheat regions of Western Europe

**S. Olin[1], G. Schurgers[1,2], M. Lindeskog[1], D. Wårlind[1,3], B. Smith[1], P. Bodin[1], J. Holmér[4], and A. Arneth[5]**

[1]Department of Physical Geography and Ecosystem Science, Lund University, 223 62 Lund, Sweden
[2]Department of Geosciences and Natural Resource Management, University of Copenhagen, Øster Voldgade 10, 1350 Copenhagen, Denmark
[3]CSIRO Sustainable Agricultural Flagship, CSIRO Agriculture, GPO Box 1666, Black Mountain, Canberra, ACT 2601, Australia
[4]Centre for Environmental and Climate Research, Lund University, 223 62 Lund, Sweden
[5]Karlsruhe Institute of Technology, Institute of Meteorology and Climate Research/Atmospheric Environmental Research, 82467 Garmisch-Partenkirchen, Germany

Correspondence to: S. Olin (stefan.olin@nateko.lu.se)

## Abstract

Nitrogen (N) is a key element in terrestrial ecosystems as it influences both plant growth and plant interactions with the atmosphere. Accounting for carbon-nitrogen interactions has been found to alter future projections of the terrestrial carbon (C) cycle substantially. Dynamic vegetation models (DVMs) aim to accurately represent both natural vegetation and managed land, not only from a carbon cycle perspective but increasingly so also for a wider range of processes including crop yields. We present here the extended version of the DVM LPJ-GUESS that accounts for N limitation in crops to account for the effects of N fertilisation on yields and biogeochemical cycling.

The performance of this new implementation is evaluated against observations from N fertiliser trials and $CO_2$ enrichment experiments. LPJ-GUESS captures the observed response to both N and $CO_2$ fertilization on wheat biomass production, tissue C to N ratios (C : N) and phenology.

To test the model's applicability for larger regions, simulations are subsequently performed that cover the wheat-dominated regions of Western Europe. When compared to regional yield statistics, the inclusion of C–N dynamics in the model substantially increase the model performance compared to an earlier version of the model that does not account for these interactions. For these simulations, we also demonstrate an implementation of N fertilisation timing for areas where this information is not available. This feature is crucial when accounting for processes in managed ecosystems in large-scale models. Our results highlight the importance of accounting for C–N interactions when modelling agricultural ecosystems, and it is an important step towards accounting for the combined impacts of changes in climate, [$CO_2$] and land use on terrestrial biogeochemical cycles.

## 1 Introduction

Nitrogen (N) plays an important role in plant productivity and physiology (Evans, 1989a) and is one of the main limiting nutrients for the functioning of ecosystems in many parts

of the world (Grindlay, 1997; Gruber and Galloway, 2008; Vitousek et al., 2002), both in natural and agricultural ecosystems. Historically in agriculture, N limitation for crops has been overcome by the use of manure and N fixing legumes (Vitousek et al., 1997). Since the discovery of the Haber-Bosch process in the 1910's, humans have been able to effectively overcome N limitation by large scale production and application of reactive N in the form of mineral fertilisers (Vitousek et al., 1997).

The enhanced input of reactive N into agricultural ecosystems by fertiliser use, and deposition to the earth's surface of nitrous oxides which are by-products from combustion, has together with other technical developments more than doubled global food production during the 20th century (Tilman et al., 2001, 2002). However, enhanced N-input can also have detrimental effects on biodiversity and water quality, and lead to substantial emissions of N trace gases that affect air quality and climate (Galloway et al., 2004; Rockstrom et al., 2009; Tilman et al., 2002; Vitousek et al., 1997). Better understanding of N effects on yields, conjointly with other ecosystem processes, especially in a changing climate and $CO_2$ environment is therefore needed for a sustainable management of agricultural ecosystems, weighing enhanced productivity against detrimental side-effects.

N cycling by ecosystems is strongly interlinked with the carbon (C) cycle, which in turn has also undergone drastic changes during the 20th century (Ayres et al., 1994; Rockstrom et al., 2009; Vitousek et al., 1997), as the increased transport of C from the geo- and biosphere to the atmosphere through various human activities leads to an increase in carbon dioxide concentration ($[CO_2]$). Higher $[CO_2]$ can have a positive effect on plant productivity, the reason for this is that $CO_2$ is the main substrate in photosynthesis. Elevated concentrations relative to $O_2$ in the intercellular spaces of leaves are known to reduce photorespiration resulting from fixation of $O_2$ by the enzyme Rubisco that catalyses the carboxylation step of photosynthesis (Long, 1991). In addition, enhanced levels of $CO_2$ result in increased water use efficiency in those plant species that lower stomatal conductance under elevated $[CO_2]$, which limits transpirational water loss (Ainsworth and Rogers, 2007; Drake et al., 1997; Sun et al., 2014). However, $CO_2$ is also a greenhouse gas that leads to higher air temperatures which in turn can either increase or decrease

plant productivity depending on the magnitude of the temperature increase. Several studies have assessed the effect that the already experienced environmental change has had on food production (e.g., Lobell et al., 2011; Olesen et al., 2011; Schlenker and Roberts, 2009; Tubiello and Ewert, 2002), and on the projected future changes, using crop models (e.g., Fischer et al., 2001; Rosenzweig and Tubiello, 2007; Rosenzweig et al., 2014). However, the magnitude of the $CO_2$ fertilisation of crop ecosystems is still under debate (Ainsworth et al., 2008; Rosenzweig et al., 2014; Sun et al., 2014).

A recent model intercomparison highlighted large uncertainties arising from treatment of warming effects vs. effects of $CO_2$ and N fertilisation on projections of global crop yields (Rosenzweig et al., 2014). In particular, differences between models, in the representation of a $CO_2$ fertilisation effect on productivity was highlighted as a key determinant of between-model differences, including globally applicable versions of traditional crop models (e.g. DAYCENT, Stehfest et al., 2007 and GEPIC, Liu et al., 2007), a crop management impact model (PEGASUS, Deryng et al., 2011) and also crop-enabled Dynamic Vegetation Models (DVMs) LPJmL (Bondeau et al., 2007) and LPJ-GUESS (Lindeskog et al., 2013).

For the simulation of crop productivity, traditional crop models typically rely on empirical scaling factors to modify the radiation-use efficiency based on measurements in $CO_2$ fertilisation experiments (Boote et al., 2013). A mechanistic representation of the $CO_2$ response (as well as other processes) has been argued to be critical when modelling crop responses to climate change (Yin, 2013), as recently shown for state-of-the-art crop models (Boote et al., 2013). In contrast to crop models, which are optimised to simulate yields, DVMs are tools for exploring and predicting the coupled dynamics of ecosystem functioning, climate-carbon cycle interactions and biome distributions (Friedlingstein et al., 2013; McGuire et al., 2001; Prentice et al., 2007). In DVMs, photosynthesis and stomatal conductance are coupled and respond conjointly to changes in $[CO_2]$ (Haxeltine and Prentice, 1996a). New developments in some DVMs in recent years are the inclusion of (1) land-use change and land management functionalities and (2) N cycling (cf., Arneth et al., 2010; Prentice et al., 2007; Smith et al., 2014; Thornton et al., 2002; Xu-Ri and Prentice, 2008).

The inclusion of N dynamics in DVMs has been found to alter future projections of climate and $CO_2$ interactions with the C cycle (Arneth et al., 2010; Friedlingstein et al., 2013; Thornton et al., 2009; Wårlind et al., 2014), while the land-use change functionality facilitates assessment of large scale patterns of changes in yields within a consistent model framework that can also address questions such as how management affects the land C sink (Bondeau et al., 2007; Lindeskog et al., 2013; Shevliakova et al., 2013). Important management options in this context include decisions on when to sow and harvest, irrigation, residue removal, presence of cover crops, tillage, or fertilisation. For the DVM LPJ-GUESS, including cropland and managed grasslands notably improved phenology when compared with satellite data (Lindeskog et al., 2013). In a study on land-use change in Africa for the 20th century, Lindeskog et al. (2013) found that the impact of implementing land-management decisions was of similar importance for the continental C budget as the effect of applying static vs. dynamic land use input data. Levis et al. (2012) showed that including an explicit representation of croplands in the Community Land Model changed both the patterns and amplitudes in the modelled climate compared to treating croplands as unmanaged grasslands. Still, only a few of today's DVMs account for crop processes and C–N coupling in crops (e.g. Arora, 2003; Drewniak et al., 2013), which is a prerequisite to accounting for fertiliser input, the associated effects it has on yields and the C cycle. These improvements will also facilitate global-scale modelling of soil processes such as nitrification and denitrification, because accounting for N uptake through plants will help to constrain ammonium and nitrate amounts, and will hence allow for modelling of soil $N_2O$ fluxes. While not the focus of this manuscript, the ultimate goal will be to assess how ecosystem fluxes affecting atmospheric composition and climate vary with changing environmental and socioeconomic conditions.

The standard version of LPJ-GUESS, which simulates potential natural vegetation, has recently been extended to include N dynamics, which has improved the model's ability to represent the biome distributions and productivity patterns globally (Smith et al., 2014; Wårlind et al., 2014). Here we complement these developments to also encompass cropland dynamics, building on the approach of Lindeskog et al. (2013),

including an enhanced temporal resolution of allocation of C and N between different plant compartments. We describe these model developments, and evaluate the model regarding the impact and uncertainty arising from differences in the timing and amount on N fertilisation. We analyse the model's ability to reproduce observed yields on different scales using data from detailed site experiments and regional wheat yield statistics in Europe as a case study. The overall aim of these developments was to find a reasonable level of complexity in processes governing physiology and management for global applications of the model.

## 2 Model description

### 2.1 LPJ-GUESS

LPJ-GUESS (Smith et al., 2001, 2014) is a DVM optimised for regional applications but also applicable globally based on a detailed individual- and patch-level representation of vegetation structure and dynamics. For global applications, vegetation is represented as a mixture of plant functional types (PFTs) that represent the globally most abundant growth strategies of woody and herbacious vegetation. PFTs are distinguished in terms of growth form, phenology, life history strategy, allometry, photosynthetic pathway ($C_3$ or $C_4$), climate-dependent scaling of physiological processes and a limited set of bioclimatic limits (Haxeltine and Prentice, 1996b; Hickler et al., 2004; Sitch et al., 2003; Smith et al., 2014). The model uses climate, [$CO_2$], soil information and N deposition as input, and plant communities evolve dynamically through competition in response to these drivers.

Recent model development includes the incorporation of land-use change dynamics together with a crop module (Lindeskog et al., 2013), further developing approaches described in Bondeau et al. (2007) and Waha et al. (2011). In the crop module for global-scale applications, the dominant crop types, such as wheat, maize and rice are represented as crop PFTs, which differ amongst others in management-related parameters such as baseline sowing and harvest dates. Sowing and harvest decisions are modelled based

on climate variability (Waha et al., 2011; Lindeskog et al., 2013) and climatic thresholds (Bondeau et al., 2007). Irrigation, residue removal after harvest and cover crops between the main growing-seasons, are further management options available in the model.

The present study builds further on LPJ-GUESS version 3.0 which includes N-cycle dynamics for the simulation of potential natural vegetation (Smith et al., 2014; Wårlind et al., 2014). Soil C and N dynamics are based on the CENTURY model (Parton et al., 1993) which represents 11 soil organic matter (SOM) and litter pools that differ in their C to N ratios (C : N) and decay rates ($K_\mathrm{d}$). Both C : N and $K_\mathrm{d}$ are dynamic within certain limits (see Smith et al. (2014) for details). SOM decomposition depends on the C : N, $K_\mathrm{d}$ as well as soil temperature and water content, and may result in either mobilisation or immobilisation of mineral N. Plant N uptake varies between PFTs which differ in their N demand and their competitive strength for N uptake. See Sect. 2.1.2 and Smith et al. (2014) for more details.

Allocation of the Net Primary Productivity (NPP) to different plant organs is done on a yearly basis, based on a set of C-allocation rules (Smith et al., 2014). If a plant experiences water or N stress during the year, the C-allocation scheme is flexibly adjusted so that a larger proportion of the assimilates are distributed to the roots to alleviate these stresses during the following year.

However, for crops, growing periods are less than one year and an annual adjustment of the allocation and growth of different plant organs is not sufficient. Lindeskog et al. (2013) partly address this issue, incorporating a C allocation that operates on a daily time step. To allow for dynamic adaptation of the allocation as a response to stress, a more detailed representation of the allocation is developed in this study (see Sect. 2.1.1).

Below we describe and evaluate an updated version of LPJ-GUESS incorporating C–N interaction also for crops. The model allocates daily NPP based on the crop's development phase and allows for an adjustment of the allocation scheme based on the current nutrient and water status of the crop.

### 2.1.1 Crop Development

Upon sowing, the development of a crop plant in LPJ-GUESS starts with a seedling that has an initial carbon mass in leaves and roots. The N content in the seedling is initiated with the highest N concentration ([N]) (the minimum C : N, C : $N_{leaf,min}$), allowed in the model assuming a seed with a high N density.

#### Development stage

In most ecosystem and crop models, plant phenological development is modelled based on weather conditions (Sinclair and Amir, 1992; Sitch et al., 2003; Smith et al., 2001; Wang and Engel, 1998; Zaehle and Friend, 2010), often accumulated over a certain time period such as heat units (HU) (Lindeskog et al., 2013; Bondeau et al., 2007). Here we define development stage (DS, Wang and Engel, 1998) as a number between 0 and 2 where: $0 < \text{DS} < 1$ is the main vegetative phase, at $\text{DS} = 1$ anthesis occurs and $\text{DS} > 1$ represents the grain filling phase. Compared to the HU implementation currently in the model, the use of DS facilitates a more detailed division of the growing period into the different crop phenological stages (Wang and Engel, 1998). Periods when the plant is more susceptible to heat and nitrogen stress can thus be represented in a more precise manner.

DS at a given point in time ($t$) is a cumulative function of the maximal development rate $d_{\text{r}}$ (day$^{-1}$) which differs between the vegetative phase ($\text{DS} < 1, d_{\text{r}} = d_{\text{r,veg}}$) and the reproductive phase ($\text{DS} > 1, d_{\text{r}} = d_{\text{r,rep}}$). Following Wang and Engel (1998), DS is also modified using dimensionless scaling factors dependent on temperature ($f_T$), vernalisation days ($f_{\text{vern}}$) and photo-period ($f_{\text{phot}}$):

$$\text{DS}_t = \text{DS}_{t-1} + d_{\text{r}} f_T f_{\text{phot}} f_{\text{vern}} \quad (1)$$

#### Daily carbon allocation

For the allocation of the plant's daily assimilates, and their partitioning to the plant organs during the growing-season, we use the established allocation scheme from Penning de

Vries et al. (1989). This scheme differs from the one implemented in Bondeau et al. (2007) and Lindeskog et al. (2013) in that the allocation of C to the different organs is related to the daily NPP and to DS, as opposed to a function that meets a predefined target at the end of the growing-season. During the first part of the vegetative phase (DS $\lesssim 0.7$ for winter wheat) most of the assimilates are used for root (R) and leaf (L) growth to maximise the uptake of water and nutrients and the absorption of radiation for photosynthesis, followed by a period when more of the assimilated C is allocated to the stem (St).

After anthesis (DS $> 1$ for winter wheat), the grain filling period starts, during which most assimilates are allocated to the storage organs. During this period, cereal crops reallocate some of their nutrients from the vegetative organs to the grains (Bertheloot et al., 2008).

When a plant experiences water or nutrient deficit during the vegetative phase, it starts to invest a relatively larger fraction of the assimilates into roots to overcome the stress (van Keulen and Seligman, 1989). It is thus important to be able to model the allocation to the roots separately from the other organs. The ratio between the allocation to leaves and stem (L : St), can be treated as constant during stress (Penning de Vries et al., 1989) and thus a relationship between the allocation to R and that to the vegetative parts ($\mathrm{V} = \mathrm{St} + \mathrm{L} + \mathrm{R}$) that is also valid under stress can be established. This approach also gives an opportunity for future implementation of dynamic adjustments in the allocation during the vegetative phase, which is lacking in the original allocation model (Penning de Vries et al., 1989).

Relationships between allocation to L, St, R and grains (Y) from the original allocation model of Penning de Vries et al. (1989) were established and fitted to a logistic growth function, a Richards curve (Richards, 1959), (Eq. 2):

$$f_i = a + \frac{b - a}{1 + e^{-c(\mathrm{DS} - d)}} \tag{2}$$

where $f_i$ is the daily allocation of assimilates to a plant organ relative to e.g. the shoot, $a$ is the asymptote when DS $\to 0$, $b$ is the upper asymptote when DS $\to \infty$, $c$ the growth rate, and $d$ is the DS of maximum growth.

**Roots**

The allocation to R ($g_{\mathsf{R}}$) relative to the vegetative organs ($g_{\mathsf{V}}$) (Eq. 3) is shown in Fig. 1a:

$$\frac{g_{\mathsf{R}}}{g_{\mathsf{V}}} = 0.52 + \frac{-0.47}{1 + e^{-7.63(\mathsf{DS}-0.55)}} = f_1 \tag{3}$$

**Leaves and stems**

Reflecting the shift from L ($g_{\mathsf{L}}$) to St ($g_{\mathsf{St}}$) allocation during the initial part of the vegetative phase as outlined above, a relationship between the two organs was derived (Eq. 4) which is illustrated in Fig. 1a.

$$\frac{g_{\mathsf{L}}}{g_{\mathsf{L}} + g_{\mathsf{St}}} = 0.88 + \frac{-0.79}{1 + e^{13.99(\mathsf{DS}-0.65)}} = f_2 \tag{4}$$

**Harvestable organs, grains**

Finally a relationship of the allocation to grains ($g_{\mathsf{Y}}$) as the fraction of the whole plant ($g_{\mathsf{Y}} + g_{\mathsf{V}}$) allocation (Eq. 5) was derived:

$$\frac{g_{\mathsf{Y}}}{g_{\mathsf{Y}} + g_{\mathsf{V}}} = \frac{1}{1 + e^{-8.32(\mathsf{DS}-1.15)}} = f_3 \Longleftrightarrow g_{\mathsf{V}} = 1 - f_3 \tag{5}$$

**Dynamic allocation**

These relationships between the allocation to the different organs of the plant can be applied to favour allocation to one organ over others. Combining Eqs. (3)–(5) yields:

$$\begin{aligned} g_{\mathsf{R}} &= f_1(1 - f_3) \\ g_{\mathsf{L}} &= f_2(1 - f_1)(1 - f_3) \\ g_{\mathsf{St}} &= (1 - f_2)(1 - f_1)(1 - f_3) \\ g_{\mathsf{Y}} &= f_3 \end{aligned} \tag{6}$$

which is illustrated for winter wheat in Fig. 1b and for spring wheat in Fig. A1b.

### Carbohydrate retranslocation

Crops store an easily mobilised reserve of carbohydrates in L, St and R (for some crops also tubers) (van Ittersum et al., 2003; Penning de Vries et al., 1989). To represent this in the model, a labile C pool is filled with a fraction of the ~~C allocated~~ daily assimilates directed to the stem ($g_{St}$), set here to 0.4 for wheat (Penning de Vries et al., 1989)~~, and thus has a cap of the allocation to stem ($g_{St}$) times 0.4~~. The labile C pool ($M_{C,labile}$) is constrained between 0 and $0.4 M_{C,St}$. During days when the daily assimilated C is lower than respiration costs (negative NPP), these sugars are used to compensate the loss (Seligman et al., 1975). Additionally, during the grain filling period the labile C pool is used to add to the grains and is reduced with a rate of 0.1 $day^{-1}$ (Penning de Vries et al., 1989).

### 2.1.2 Daily nitrogen allocation

During the vegetative phase in which the leaves and roots are expanding, the plant seeks to maximise photosynthetic gain by having a leaf N content that optimises the carboxylation capacity ($V_{max}$) (Hirose and Werger, 1987; Kull, 2002). Following Haxeltine and Prentice (1996a) and Smith et al. (2014) this is done by calculating the $V_{max}$ that maximises canopy-level net C assimilation given the current temperature, water status and biomass C : N.

### Leaf N content

Nitrogen associated with Rubisco, the key enzyme in photosynthesis, makes up more than 20 % of the total N in the leaves of wheat (Evans, 1989a), but N is also important for plant structural tissues (Anten et al., 1995; Hirose, 2005; Kull and Jarvis, 1995). However, the vertical distribution of N in the canopy is not even. Higher [N] is usually found in the upper part of the canopy, where leaves experience the highest levels of irradiance (Hirose and Werger, 1987; Hollinger, 1996; Evans, 1989b), compared to the more shaded leaves below. The decline in leaf [N] with the increase in cumulative leaf area index (LAI) from top to bottom typically follows an exponential decrease with a N extinction coefficient $k_N$ that is

related to the light extinction coefficient ($k_{\mathrm{L}}$) as follows:

$$k_{\mathrm{N}} = \beta_0 + \beta_1 k_{\mathrm{L}} \tag{7}$$

where $\beta_0$ and $\beta_1$ are regression coefficients taken from Yin et al. (2003). From theory on optimal N distribution in a crop canopy, Yin et al. (2000) derived a relationship between the LAI that can be supported given the amont of N that is currently in the leaves ($\mathrm{LAI_N}$) and $\mathrm{k_N}$:

$$LAI_N = \frac{1}{\mathrm{k_N}} \ln(1 + \mathrm{k_N} \frac{M_{\mathrm{N,L}}}{\mathrm{N_b}}) \tag{8}$$

where $M_{N,L}$ is the leaf N mass and $\mathrm{N_b}$ (Eq. 9) is the minimum N requirements for the leaf to function.

$$\mathrm{N_b} = \frac{1}{\mathrm{C:N_{L,max}SLA}} \tag{9}$$

where $\mathrm{C:N_{L,max}}$ reflects the minimum N required for photosynthesis and SLA is the specific leaf area ($\mathrm{m^2\ kgC^{-1}}$). $\mathrm{LAI_N}$ is then compared to LAI to determine the N status of the canopy, see Sect. 2.1.3.

**Root N content**

The N requirement of the root follow that of the leaves through the functional balance concept (van Ittersum et al., 2003; Smith et al., 2014; Zaehle and Friend, 2010):

$$\frac{M_{\mathrm{N,L}}}{M_{\mathrm{C,L}}} \propto \frac{M_{\mathrm{N,R}}}{M_{\mathrm{C,R}}} \tag{10}$$

where $M_{\mathrm{N,L}}$ denotes leaf N mass, $M_{\mathrm{C,L}}$ leaf C mass, $M_{\mathrm{N,R}}$ root N mass and $M_{\mathrm{C,R}}$ root C mass. The theory behind the concept is that the activity of the roots (uptake and transport of water and nutrients) is proportional to that of the leaves (photosynthesis). A high photosynthesis rate in the leaves (high $[\mathrm{N}]_{\mathrm{L}}$) implies a corresponding relative [N] in the roots to supply the demand of the leaves (Smith et al., 2014; Zaehle and Friend, 2010).

### Plant N uptake

Following Smith et al. (2014), plants take up N from the mineral N pool in the soil on a daily time-step as the lesser of the plant demand versus the amount of mineral N in the soil accessible for the plant. N demand from leaves and roots depend on their current C : N status, tas the plant seeks to reach optimal C : N in leaves and roots. The mineral N accessible for the plant, depends on soil temperature and fine root biomass: see Smith et al. (2014) and Zaehle and Friend (2010) for details. For crops, we have expanded the soil N module so that the N available for uptake by the plant ($M_{\text{N,avail}}$) is related to the water content of the soil (Eq. 11), as proposed by Xu-Ri and Prentice (2008):

$$M_{\text{N,avail}} = \theta \varphi M_{\text{N,soil}} \tag{11}$$

where $\varphi$ is the fraction of projected leaf coverage by the plant (proportional to the fine root area), $M_{\text{N,soil}}$ is the mineral N mass of the soil and $\theta$ is the mean water content of the soil profile.

## 2.1.3 Senescence

Senescence, the killing of cells, can be either genetically programmed and age dependent, or induced by stresses or environmental factors (Thomas and Stoddart, 1980). In the C-only original cropland version of LPJ-GUESS (Lindeskog et al., 2013), leaf senescence is a function of HU (see Sect. 2.1.1). We develop this further here with a dynamic response of plant senescence to its N status (Yin et al., 2000; Masclaux-Daubresse et al., 2010) and age (DS).

### Leaf senescence

If the N status of the leaves is suboptimal, the plant tries to maximise the leaf N in the canopy by redirecting some of it from the shaded leaves towards those that are more sunlit (Hirose and Werger, 1987; Yin et al., 2000). This will eventually turn off the photosynthetic

apparatus in the leaves from which all the non-structural N has been retranslocated (Thomas and Stoddart, 1980). Senescence of part of the canopy in the model is induced when the N-determined leaf area index $\mathrm{LAI_N}$ (Eq. 8) (Yin et al., 2000) is lower than the actual LAI (Eq. 12):

$$\mathrm{LAI} = M_{\mathrm{C,L}}\mathrm{SLA} \tag{12}$$

where $M_{\mathrm{C,L}}$ is the total C mass of the green leaves. For plants, senescence of leaves is not an instantaneous process. The time for the acclimation of the N content in crop leaves was estimated to be around 10 days (Seligman et al., 1975) which is within the range of what is observed for natural vegetation, 5–30 days (Kull, 2002). Implemented here is the proposed reduction of the leaf C mass as in Yin et al. (2000) $m_{\mathrm{C,sen}}$ but with an inertia of 0.1 $\mathrm{day}^{-1}$:

$$m_{\mathrm{C,sen}} = 0.1\frac{\mathrm{LAI} - \min(\mathrm{LAI},\mathrm{LAI_N})}{\mathrm{SLA}} \tag{13}$$

The leaf C mass is then updated $M'_{\mathrm{C,L}} = M_{\mathrm{C,L}} - m_{\mathrm{C,sen}}$ and N accordingly using the minimum N content of the leaves, $\mathrm{C:N_{L,max}}$, $M'_{\mathrm{N,L}} = M_{\mathrm{N,L}} - m_{\mathrm{C,sen}}\mathrm{C:N}^{-1}_{\mathrm{L,max}}$. The senesced C and N is then transferred to a pool of dead leaves with a high C : N, currently set to 100 (van Ittersum et al., 2003) and the residual N is translocated to ~~then~~ the labile N pool. In contrast to the labile C pool, ~~there is no explicit cap on this pool , but the~~ N allocated to the labile pool is not determined as a fraction of the total allocation. The amount is constrained ~~since leaves and roots act as labile N sources.~~by the N translocated from senesced leaves (Eq. 14) and roots accordingly through the functional balance concept (Eq. 10). The N that is translocated to the labile N-pool due to senescence of the leaf is the leftover after maximising the $\mathrm{C:N_L}$ status:

$$m_{\mathrm{N,sen}} = \begin{cases} M'_{\mathrm{N}} - \frac{M'_{\mathrm{C,L}}}{\mathrm{C:N_{L,opt}}} & \text{for } \mathrm{C:N_L} < \mathrm{C:N_{L,min}} \\ 0 & \text{for } \mathrm{C:N_L} \geq \mathrm{C:N_{L,min}} \end{cases} \tag{14}$$

where $C:N_{L,opt}$ is the $C:N$ below which a decrease has a small or no effect on photosynthesis which is estimated here as $3/4$ of the range between $C:N_{L,max}^{-1}$ and $C:N_{L,min}^{-1}$.

In ageing leaves, observed enzyme efficiency is reduced. After anthesis, degradation of the enzyme Rubisco is higher than the de novo synthesis (Bertheloot et al., 2008). To reflect this in the model, a reduction of the leaf N content at rate of $0.1\,\mathrm{day}^{-1}$ (Bertheloot et al., 2008) starts at anthesis ($DS > 1$).

In order to avoid excessive allocation of C to the leaves while the plant experiences leaf-N deficit ($m_{C,sen} > 0$) during the vegetative phase, a rescaling of the factor that controls the flow of assimilates to the leaves ($f_2$, Eq. 4) was implemented:

$$f_2' = (f_2)^2, \text{ for } m_{C,sen} > 0 \tag{15}$$

**Root senescence**

Root senescence is still an unexplored area (Kunkle et al., 2009). In the absence of a full mechanistic understanding, the dynamics of the root in the model are assumed to be coupled to those of the leaves through the functional balance concept (Eq. 10).

### 2.1.4 Seed development

During flowering and grain filling, a fraction of the assimilates is allocated to the grains, while the N transported to the grains comes primarily from the leaves (Seligman et al., 1975; van Keulen and Seligman, 1989). This is reflected in the model as a transport of N from the leaves, roots and the labile N pool. In the model the plant tries to meet the demand from the grain:

$$m_{N,Y,dem} = \frac{m_{C,Y}}{C:N_{L,min}} \tag{16}$$

primarily by reducing the labile N pool, $M_{N,labile}$.

### Nitrogen retranslocation

If $m_{\mathrm{N,Y,dem}}$ is larger than the labile N pool, the crop plant attempts to meet the unsatisfied N demand from the grains ($m'_{\mathrm{N,Y,dem}} = m_{\mathrm{N,Y,dem}} - M_{\mathrm{N,labile}}$) by a N transport from the donor organs (leaves and roots). These donor organs have a resistance to let go of their N, $r$ (Seligman et al., 1975), to account for the fact that N is needed for maintaining organ processes (e.g. photosynthesis and maintenance respiration):

$$r_j = \left(1 - \frac{\mathrm{C:N}_{j,\mathrm{opt}}^{-1} - \mathrm{C:N}_{j}^{-1}}{\mathrm{C:N}_{j,\mathrm{opt}}^{-1} - \mathrm{C:N}_{j,\mathrm{min}^{-1}}}\right)^2, r \in [0,1] \tag{17}$$

where $j$ denotes the organ, L or R. The actual transport of N ($m_{\mathrm{N,retr}}$) is calculated by summing the individual organs' relative portion of the total N demand from the grains after the labile pool has been emptied (Eq. 18). If the demand on the organ is larger than the available N, it is reduced to its minimum N content ($\mathrm{C:N}_{j,\mathrm{max}}$).

$$m_{\mathrm{N},j,\mathrm{retr}} = \min\left(\frac{M_{\mathrm{C},j}}{\mathrm{C:N}_{j,\mathrm{max}}}, \frac{m'_{\mathrm{N,Y,dem}}(1-r_j)}{1-r_{\mathrm{L}}+1-r_{\mathrm{R}}}\right) \tag{18}$$

During the initial part of the grain filling period, only leaves contribute to fulfilling the grain N demand. Once more than half of the assimilates goes to the grain (DS $> 1.15$, see Eq. 5), the model can utilize part of the plant root N as well to fulfill the N requirements of the grains.

### 2.1.5 Updated soil water parameters

Soils are characterized by their ability to store and provide water to the plants; a parameterization of these soil water characteristics based on fractions of grain sizes, available for the soils in the study area, was needed for this study. Soil water characteristics as used in LPJ-GUESS were derived from data on sand, silt and clay for the top soil layer taken from a map of soil mineral fractions. These fractions were then used as input to empirical relationships (Cosby et al., 1984, Table 3) for the following soil water

characteristics: soil water pressure at saturation ($\Psi_s$), volumetric water content at saturation ($\theta_s$) and a shape parameter describing the response of the water retention curve to changes in water content ($b$). These parameters were then used in Eq. (19) to derive the volumetric water content under specific conditions:

$$\Psi_i = \Psi_s \left(\frac{\theta_i}{\theta_s}\right)^b \Longleftrightarrow \theta_i = \theta_s \left(\frac{\Psi_i}{\Psi_s}\right)^{-b} \tag{19}$$

where $\Psi_i$ is the actual pressure head (m) and $\theta_i$ is the actual volumetric water content ($m^3\ m^{-3}$).

The percolation coefficient $K$ (Haxeltine and Prentice, 1996b; Gerten et al., 2004), an empirical parameter used in the model to derive the daily percolated water, was fitted against $b$ values for 4 of the soil classes from Haxeltine and Prentice (1996b) (coarse, medium-coarse, medium, fine) and resulted in:

$$K = 5.49 - 0.22b \tag{20}$$

## 3 Experimental setups

The model's ability to simulate yields was evaluated using data from fertiliser trials from the Netherlands, a Free Air $CO_2$ Enrichment (FACE) experiment from Germany and regional yield statistics from European countries.

All simulations were performed using a 500 year spin-up using [$CO_2$] and repeatedly cycled detrended climate input for the first years of the historic climate data to build up pools of C and N. In the simulations with N dynamics turned on, monthly N deposition input from Lamarque et al. (2010) that varies decadally was used. The values were interpolated using bilinear interpolation from the original resolution ($1.9^\circ \times 2.5^\circ$) to match the resolution of the climate data ($0.5^\circ \times 0.5^\circ$) (Smith et al., 2014; Wårlind et al., 2014).

### 3.1 Fertiliser trials

~~The simulated growth response to added N depends on several processes in the model (represented by e.g. Eqs ...).~~ To evaluate the model's ability to simulate phenology and yields, and sensitivity to N fertiliser additions, data from nitrogen fertiliser response trials with detailed measurements of dry mass and N mass allocation from the Netherlands (Groot and Verberne, 1991) were used. In the trials, winter wheat was grown with different fertiliser input in the years 1983–1985. The trials were conducted on three sites (The Eest, The Bouwing and PAGV), located in the central part of the Netherlands, see Fig. A2. At these locations, three different N treatments were carried out for two seasons (Table 1).

Based on an initial calibration of the model using leaf phenology data from Trial I, the parameters $a$ and $b$ in the allocation function $f_2$ (Eq. 4) were changed from 0.88 and 0.09 to 0.8 and 0.2 respectively, for this application. Daily climate data for the years 1979 to 1984 were downloaded from the Haarweg weather station, Wageningen University[1], located within 70 km from the sites. To initialise (spin up) N and C pools in the model, climate data for the year 1979 were repeated for 500 years. In Groot and Verberne (1991), there is no information on management practices in previous years, so we decided to implement a moderate level of 100 kg N $ha^{-1}$ $y^{-1}$ as a single application, 150 days after sowing for the spinup. The year before the trials started (1982 for Trials I, III and V and 1983 for Trials II, IV and VI) 200 kg N $ha^{-1}$ was applied, following Groot and Verberne (1991, ,Table 1). As described in Sect. 2.1.5, fractions of sand, silt and clay from Table 1 were used to derive site specific soil water characteristics.

### 3.2 FACE experiment

The ability of the model to simulate the observed response to elevated [$CO_2$] treatment on yields and C : N of cropland ecosystems was tested using a FACE experiment (Weigel and Manderscheid, 2012) from an experimental site close to Braunschweig, Germany (10.83° E, 52.82° N), see Fig. A2. Between the years 1999 and 2005 the FACE experiment was carried out on a rotation of barley, ryegrass, sugar beet and winter wheat that was repeated once. At

[1] http://www.met.wau.nl/haarwegdata/dayfiles/, last access: 4 February 2014

this point the N-enabled model is not equipped to model crop rotations or sugar beet. Also LPJ-GUESS does not model wheat and barley explicitly, but temperate cereals (Bondeau et al., 2007; Lindeskog et al., 2013) represented by wheat (spring and winter) in the model, therefore growth of cereals was simulated for all years.

Four different trials from the experiment were simulated, high (100 % N) and low (50 % N) N input with ambient and elevated [$CO_2$] (378/548 ppm), see Table 2 or Table 1 in Weigel and Manderscheid (2012) for more details. Due to the lack of information on the timing and amount of the individual fertiliser applications, these parameters were set using the results from the regional comparison (Sec. 3.3), total amount of N added in the experiments are listed in Table 2. As climate input we used the WFDEI climate dataset (Weedon et al., 2012) which is a bias-corrected reanalysis dataset based on WATCH (Weedon et al., 2011) and Era Interim (Dee et al., 2011). During the spin up period (500 years), 30 years of detrended data (1979–2008) were used together with the ambient [$CO_2$] from 1979.

### 3.3 Regional yields

To evaluate the model's ability to simulate wheat yields on a larger scale, 65 regions at the NUTS2 (Nomenclature of Territorial Units for Statistics in the EU; statistical administrative areas) level from north western mainland Europe and NUTS1 for southern England were selected based on their cereal fractions and yields taken from the EU statistics website, EUROSTAT[2]. The regions and their administrative names are shown in Fig. A2 and the mean reported yields together with the number of years for which there where data for each region are listed in Table A3.

As climate input, WFDEI (Weedon et al., 2012), with a spatial resolution of $0.5^\circ \times 0.5^\circ$ was used. Spin-up with climate and [$CO_2$] was performed as in the FACE experiment (see above). Soil characteristics (mineral size distributions) for the top layer (0.3 m) were derived from Batjes (2005) and used for the whole column (2 m). Simulated yields of spring and winter wheat were assigned to the regions by their relative proportion of the grid-cell area

[2]http://epp.eurostat.ec.europa.eu/portal/page/portal/agriculture/data/main_tables, last access: 6 May 2014

(a grid-cell can belong to more than one region). Fractions of each grid-cell covered by spring and winter wheat as well as the area equipped for irrigation were derived from the MIRCA data set (Portmann et al., 2010).

Timing of the fertiliser applications were selected based on the mean development stages for the three N applications listed in Table 1, (0.18, 0.49, 0.89). A common practice is to apply some or all of the fertiliser at the time of sowing (Mahler et al., 1994). The timing of the three applications was therefore changed to DS $= 0$, 0.5 and 0.9 respectively.

To test the effect of timing and amount of fertiliser applied, an experiment with 50 model permutations ($F_{\mathrm{T,A}}$, timing (T) and application (A) varied), was conducted with five different fertiliser application rates (between 50 kg N $\mathrm{ha}^{-1}\,\mathrm{y}^{-1}$ and 250 kg N $\mathrm{ha}^{-1}\,\mathrm{y}^{-1}$). Fractions (0, $1/3$, $2/3$, 1) of the applied N were distributed at the development stages 0, 0.5, and 0.9, yielding 10 possible combinations.

The N managements (application rate and timing) that gave the best fit (lowest RMSE) were then selected for each region ($F_{\mathrm{opt(T,A)}}$). To test whether a mean N management can be representative for the whole region, the mean timing and amount from $F_{\mathrm{opt(T,A)}}$ were derived and simulated ($F_{\mathrm{t,a}}$, timing (t) and application (a) fixed). Additionally, to test the relative importance of timing and amount, an experiment with simulations where timing was fixed using the mean development stages as in $F_{\mathrm{t,a}}$ together with varying input as in $F_{\mathrm{T,A}}$ ($F_{\mathrm{t,A}}$) and an experiment where timing was varied as in $F_{\mathrm{T,A}}$ but with a fixed N application, were performed ($F_{\mathrm{T,a}}$). Furthermore a simulation using a gridded data set of annual N input for wheat (Elliott et al., 2014) together with the mean timing from $F_{\mathrm{t,a}}$ was performed ($F_{\mathrm{t,I}}$).

To test whether adding C–N dynamics in the model increased the overall model performance, simulations using the C only version of LPJ-GUESS were performed ($F_{\mathrm{C}}$). In these simulations, C allocation was as described in Lindeskog et al. (2013).

A short description of the model setups used, together with their abbreviations, are listed in Table 3.

### 3.4 Statistical methods

In order to quantify the degree of agreement between simulations and the associated observations, two indices were calculated, the Willmott index of agreement ($W_{\text{i}}$, Eq. 21) (Willmott et al., 2012) and the root mean square error (RMSE) (Eq. 22). $W_{\text{i}}$ is calculated as:

$$W_{\text{i}} = \begin{cases} 1 - \frac{M}{cO} & \text{for } M \leq O \\ \frac{cO}{M} - 1 & \text{for } M > O \end{cases} \tag{21}$$

where $M$ denotes the sum of absolute differences between the modelled and the observed mean and $O$ is the sum of absolute differences between the observations and the observed mean and $c$ is scaling constant here set to 2 (Willmott et al., 2012). $W_{\text{i}}$ is without unit and ranges from 1 to $-1$, where 1 is a perfect agreement between the modelled and observed variances and $-1$ means that there is a low or no agreement between the modelled and observed variances. RMSE is calculated as:

$$\text{RMSE} = \sqrt{\frac{\sum_{i=1}^{n} (o_i - m_i)^2}{n}} \tag{22}$$

where $n$ is the number of observations, $o$ is the observed value and $m$ is the modelled value.

### 3.5 Conversion factors

To convert plant C to total dry matter, a conversion factor of 0.446 was used (Osaki et al., 1992). Dry weight was converted to wet weight (used in the regional statistics) by assuming a wet fraction of 0.15 in the grains (Fader et al., 2010).

## 4 Results

### 4.1 N fertiliser response

In the N fertiliser experiments from Groot and Verberne (1991), 18 trials with N input ranging from 0 to 240 $\mathrm{kg\,N\,ha^{-1}\,y^{-1}}$ applied at various crop development stages were performed, resulting in grain C production from 1 to 3.5 $\mathrm{ton\,C\,ha^{-1}}$. During the growing-season, leaf C in the field trials increased until peaking around June, after which senescence commenced and leaf C decreased again (Fig. 2a–c). Simulations with LPJ-GUESS at these sites, and reproducing the applied fertiliser scheme broadly captured these seasonal dynamics, and the response to the different levels of N applications (Fig. 2a–c). Modelled grain and above-ground C mass per kg N applied (19 and 46 $\mathrm{kg\,C\,kg\,N^{-1}}$) were in line with the observed response of 22 and 42 $\mathrm{kg\,C\,kg\,N^{-1}}$, which indicates appropriate sensitivity of yield and growth to nitrogen addition. Differences between simulated and observed leaf C values were largest towards the end of the growing-season (Fig. 2d), especially at the highest-fertilised trial sites and in the second growing-season. As seen from the example time series in Fig. 2a–c, rates of senescence in the simulations were too slow, compared to measurements, which resulted also in underestimated dead-leaf C (see Fig. A3a–b).

The model generally simulates the observed above-ground production of biomass (C and N) well at the sites, with more accuracy in the medium and high input trials (2 and 3) (Fig. 3c–d). C content in grains and above-ground biomass is captured reasonably well, with some underestimations for the lowest N trial (Fig. 3c). This picture was mostly similar also for simulated N content, as a consequence average C : N were not biased towards too high or too low values (Fig. 4a). The C : N of the grains (Fig. 4b) in response to differences in N treatment was better captured than the total C mass (Fig. 3c). Over the growing-season there is an underestimation of the N content in the grains, especially so for the low input treatments (Fig. 3a–b).

## 4.2 Response to elevated $[CO_2]$

At the Braunschwieg FACE experimental site the mean observed yields under ambient $[CO_2]$ ($\sim 378$ ppm) were 8 and 6 ton ha$^{-1}$ for the sufficiently fertilised (100 % N) and the treatment receiving 50 % N respectively, whereas the simulated yields were 9 and 7 ton ha$^{-1}$, with the same pattern of higher simulated than observed yields also for the elevated $[CO_2]$ ($\sim 548$ ppm) treatments (Fig. 5).

Grain yields were simulated to rise by 19 % as a response to elevated $[CO_2]$ for both the 100 and 50 % N treatments (Fig. 5). The observations show a similar response with a rise of 14 % ((9–19 %) for 100 % N and (5–24 %) for 50 % N), and neither simulations nor measurements did indicate a clear impact of N treatment on the $CO_2$ effect.

Under elevated $[CO_2]$, increased C sequestration and yields were not balanced by grain N rising at the same rate as grain C, leading to enhanced grain C : N at elevated $CO_2$. In the observations, this increase was on average 16 % for both N treatments, whereas in the simulations the increase was 24 % (100 % N) and 20 % (50 % N) (Table 4).

## 4.3 Regional wheat yields

In order to test model performance on spatial scales beyond field trials, regional modelled wheat yields were compared with yield statistics provided by EUROSTAT. The simulations were also set up to test the effects of different N management regimes (Table 3) in order to derive an implementation of fertiliser application that can be adopted for large-scale models even when exact information on fertiliser timing is not available.

To do so, from the 65 regions chosen from the EUROSTAT database, a set of 50 permutations of timing and amount of N application ($F_{\mathrm{T,A}}$) was used to identify the management strategy resulting in the best agreement (lowest RMSE) with reported time series of yields ($F_{\mathrm{opt(T,A)}}$). The optimised timing and associated amount of N input for each of the regions are listed in Table A3. This "optimised" simulation deviated only marginally (Fig. 6b) from the observed yields (Fig. 6a). The interannual variability in yields for individual regions was captured best for regions with a low productivity (model performance based on

the Willmott index ($W_i$) and RMSE, Table A3), whereas the interannual variability for the more productive regions was captured less well.

In the optimised simulation ($F_{\text{opt(T,A)}}$), the mean N application rates for spring-sown wheat across the entire region were a total of 129 kg N $ha^{-1}$ $y^{-1}$, applied in fractions of 0.11, 0.50 and 0.39 at the three development stages described in Sect. 3.3, with the main application in mid-spring. For winter wheat, on average 172 kg N $ha^{-1}$ $y^{-1}$ were applied with fractions 0.08, 0.19 and 0.73 for the three development stages, with the main application in late spring or early summer.

For simulation $F_{\text{t,I}}$, the mean timing obtained from the optimisation was combined with a gridded data set of N application rates (Elliott et al., 2014), resulting in a reasonable agreement with the observed yield but with larger spread compared to $F_{\text{opt(T,A)}}$ (Fig. 6c). In particular, overestimations were found in parts of the Netherlands, Belgium and southwestern France, and a considerable underestimation in northern France. Some of the deviations between modelled and reported yields were likely due to a lack of spatial variability in the fertiliser data input, e.g., a constant value (110 kg N $ha^{-1}$ $y^{-1}$) was applied for all regions in France (Table A3).

Despite the spread between the model and the observations for individual years, the temporal average of the optimised set showed a good agreement (Fig. 7). Even the simulation that applied the mean timing with reported fertiliser rates ($F_{\text{t,I}}$) showed a reasonable agreement, but generally overestimating the yields in low-productive areas, primarily because of a higher fertiliser application rate (regional mean N input of 188 kg N $ha^{-1}$ $y^{-1}$ for $F_{\text{t,I}}$, compared with 169 kg N $ha^{-1}$ $y^{-1}$ for $F_{\text{opt(T,A)}}$). Applying the same timing as in $F_{\text{t,I}}$ with the lower constant rate of 169 kg N $ha^{-1}$ $y^{-1}$ ($F_{\text{t,a}}$) resulted in a much better agreement for the mean response. However, both simulations ($F_{\text{t,I}}$ and $F_{\text{t,a}}$) have a smaller range of simulated yields from low-productive to high-productive areas than reported in the statistics data.

The spatial variation of the observations was captured well in all simulations except for those with maximised yields (max($F_{\text{T,A}}$)) and the C-only version ($F_{\text{C}}$). As expected, optimised N management ($F_{\text{opt(T,A)}}$ and $F_{\text{t,A}}$) improved the fit of the model results to spatial

variation in the data, but all the C–N enabled simulations except for max($F_{T,A}$) increased the agreement between the modelled and observed variance (Table 5), when compared to $F_C$. In order to address the spatial variability in timing and rates of fertiliser application, the optimised simulation ($F_{opt(T,A)}$, red line in Fig. 7) was compared with two additional optimisations. In the first of these ($F_{opt(t,A)}$), timing was prescribed using the same as for $F_{t,a}$ while application rates were varying. In the second optimisation ($F_{opt(T,a)}$), application rates were prescribed as for $F_{t,a}$ while timing was varying. The grid cell average yield over the region and all permutations in the $F_{opt(T,A)}$ simulations was 5.2 ton. ha$^{-1}$ y$^{-1}$, ranging from 2.4 to 10.3 ton. ha$^{-1}$ y$^{-1}$ between the different application rates and timing. For $F_{opt(T,a)}$ the same measures were 5.5 ton. ha$^{-1}$ y$^{-1}$ (3.1–8.7 ton. ha$^{-1}$ y$^{-1}$) and for $F_{opt(t,A)}$, 5.2 ton. ha$^{-1}$ y$^{-1}$ (3.2–8.6 ton. ha$^{-1}$ y$^{-1}$). The average yields for all simulations were of the same order of magnitude. For $F_{opt(t,A)}$ and $F_{opt(T,a)}$ the ranges in yield were also of similar size whereas the range for the $F_{opt(T,A)}$ was larger although smaller than the sum of the ranges of $F_{opt(t,A)}$ and $F_{opt(T,a)}$. Most importantly, both the optimisations with either fixed timing or application rate, resulted in a better agreement with the reported yields than when only using a mean uniform N management over the region ($F_{t,a}$, Table 5), but optimising the application rates gave a considerably better fit than optimising the timing. While timing had a large effect, these results imply that highest priority is to obtain data on application rates.

## 5 Discussion

Accounting for C–N dynamics in the crop version of LPJ-GUESS (Lindeskog et al., 2013) together with the new flexible allocation scheme resulted in good overall agreement when compared against site-scale observations and regional yields statistics. The simulated response to N management was also in line with the observed dynamic responses in a fertiliser trial and wheat grown under elevated [$CO_2$].

### 5.1 Model performance, fertiliser trials

Modelling the seasonality of growth, phenology, and the response to fertiliser is a prerequisite not only for model projections of crop yield responses to management in a changing environment, but also to aid assessments of management-related detrimental effects (Hawkesford, 2014; Lokupitiya et al., 2009). Models that operate on regional to global scales are not designed to be suitable tools for detailed local-scale decision-making on fertiliser use, but the improved representations of crop C–N coupling and phenology are necessary for simulating regional to global land use related surface-atmosphere exchange fluxes, to evaluate models against observations, and to contribute to analyses of the effects of land-use change in the climate system, including assessment of how multiple ecosystem-services are affected following land conversions (e.g., Kelley et al., 2013; Rounsevell et al., 2014). For these types of questions, a chief challenge remains in representing phenology and growth responses to fertiliser application and climate in a way that is suitable for large-scale models, but still reproduces realistic results (Boote et al., 2013; Lokupitiya et al., 2009).

In LPJ-GUESS, crop phenological events, and especially the growth of the leaves throughout the growing-season were captured (Fig. 2) and at the end of the growing-season, senescence was induced as a result of N retranslocation to grains from the leaves, albeit with a response that was a little too weak compared to the measurements (Fig. 2). The modelled mean harvest index ($HI = Y/(Y + V)$) of 0.57 was in line with the value obtained from observations (0.52; Fig. 3a,c). Modelled grain yields and above-ground biomass were on average only slightly lower than the observations, and the overall tissue as well as grain C : N also agreed well with the corresponding ratios derived from the measurements. But there was a discrepancy in the modelled C allocated to the grains during the early parts of the grain filling period that disappeared towards the end of the growing period (Fig. 3a).

When making these comparisons, the need to convert dry matter to mass of C, and vice versa, added a level of uncertainty that is not associated with modelled processes, since site-data often is reported as biomass (dry or wet). For instance, we used the published

observations of [C] in the biomass of 44.6 % (Osaki et al., 1992) when converting the experimental-site data. By contrast, in LPJ-GUESS a C content of 50 % is assumed (Smith et al., 2014), which leads to slightly higher C density in modelled output compared to the observation-derived values.

Underlying the good agreement of the tissue C : N, was an underestimation of the absolute levels of both C and N in the grains at the end of the growing-season, which were underestimated by about 30 % in many cases (Fig. 3a). The same pattern could also be seen for the above-ground C mass (Fig. 3c), suggesting that the productivity generally is too low in the model. One potential explanation for the underestimation of [C] in grains at the end of the growing period is C-retranslocation from leaves and roots to the grains during the growing-season, which has been observed, in forms of sugars (Osaki et al., 1991; Penning de Vries et al., 1989). Since in the current version of the model C supply originates solely from NPP, one potential source of carbon to grain filling therefore is missing. In addition, the model does not presently include other forms of molecular transport whereas the re-translocation of N from leaves to the grains is mostly in the form of amino-acids (van Keulen and Seligman, 1989) with a relatively low C : N (e.g. 4.0 in wheat Thornley, 1990; Osaki et al., 1991). Accounting for such an amino-acid transport would suggest that for every unit of N that is transported to the grain, four C would have to be supplied as well. This, too, cannot be captured by the current implementation that is based on allocation of the daily NPP.

Since the C : N of the various organs plays an important role for determining N uptake and its N (re)allocation between organs, variable C : N have been suggested to be crucial when modelling vegetation C–N dynamics. This aspect might become especially important under changing climate and [$CO_2$] environments (Yin and Struik, 2010) as these can affect the chemical composition of the plant (e.g., Ainsworth and Long, 2005; Yin, 2002), discussed in Sect. 5.2. For present-day conditions, the simulated biomass C : N agreed best with observations from the two high N input treatments (2 and 3) (Fig. 4), although the overall agreement across treatments was acceptable, keeping in mind the assumptions that had to be made when deriving the observation-based values. Likewise, growing-season green leaf

[N], which together with LAI is essential for predicting photosynthesis (Boote et al., 2013), was also well reproduced (results not shown). By contrast, [C] as well as [N] in the dead leaf pool were either over- or underestimated (see Fig. A3), most likely because the C : N in dead leaves is set to a constant value.

Tissue C : N in dead leaves will affect C and N input to the soil through litter decomposition, and hence is arguably an important feature for representing the N cycling in ecosystems. We concentrate here on aboveground processes such as live-tissue growth, element concentrations and yields and it remains to be tested whether an implementation of C : N limits that vary over the course of the growing-season (Asseng et al., 2004) will be a necessary improvement for simulating agricultural soil processes. Moreover, a dynamic adjustment of the C and N allocation to root growth under stress (see Sect. 2.1.1) might be an important future development, since as a result, less C would be partitioned towards above-ground growth while at the same time, more N could be extracted from the soil. For the observations used here for model evaluation, no data are available on the N or C content of the roots. A flexible adjustment of the root:shoot growth is already implemented in the model as a response to N and water stress for natural vegetation, but it operates so far only on a yearly basis (Smith et al., 2014). Studies elsewhere have demonstrated dynamically adjusted shoot : root growth and C : N (Poorter et al., 2012), and some published crop models like GECROS (Yin and Van Laar, 2005) do so at higher temporal resolution. Next development phases in LPJ-GUESS will explore how to include these into the model.

### 5.2 Model performance, FACE comparison

In a recent intercomparison of crop models that can be applied globally, Rosenzweig et al. (2014) identified the $CO_2$ fertilisation response to be one of the major sources of uncertainty of how yields might change in a future environment. When disregarding advances in breeding, the $CO_2$ fertilisation response of crops (in particular: of the $C_3$ photosynthesis-type) is fundamental, as this response can counteract or at least dampen effects of climate change. The chief principles are related to the carboxylation reaction of Rubisco being stimulated by enhanced levels of $CO_2$, and by plants being able to operate at lower levels of

stomatal conductance, thereby increasing the efficiency of gaining carbon per unit of water lost (Ainsworth and Rogers, 2007; Drake et al., 1997; Sun et al., 2014). The magnitude of the positive $CO_2$ response on yields will depend on the degree of leaf-level acclimation response, and how such an acclimation would translate to the whole-plant level (Ainsworth and Long, 2005; Drake et al., 1997; Smith and Dukes, 2013).

In existing crop models, the implemented $CO_2$ response is typically based on empirical relationships between an increase in [$CO_2$] and plant productivity, derived from e.g. FACE experiments (Boote et al., 2013; Rosenzweig et al., 2014). Adapting a more mechanistic representation of the $CO_2$ response by replacing a radiation-use efficiency formulation with a coupled photosynthesis and stomatal conductance description (as in LPJ-GUESS) increased the overall model performance of the DSSAT model and its ability to capture responses to the combined effects of different factors affecting plant productivity (Boote et al., 2013).

In the Rosenzweig et al. (2014) study, LPJ-GUESS showed a very strong yield response to enhanced levels of atmospheric $CO_2$. The model version used in that study did not include C–N interactions, and hence this strong response was expected, since the simulated underlying physiology was not constrained by N availability. With this constraint in place, LPJ-GUESS in the present study reproduced crop growth and productivity under elevated [$CO_2$] with different N fertiliser treatments, as well as responses in dry matter C : N observed at the different levels of $CO_2$, with C : N at the 100 % N treatment being somewhat above the observed values. A positive $CO_2$ effect on yields and C : N, as well as the higher variability between years was captured in treatments that received less N input. The results shown in Sect. 4.2 were also in line with observations from previous FACE experiments (Ainsworth and Long, 2005) that showed a mean increase of 14 % ($-2$ to 33 %) for wheat yields, compared to the modelled response of 20 and 24 % for the two different N treatments.

The modelled yields (ambient and elevated [$CO_2$], 50 and 100 % N) exceeded observations only slightly. This might be explained by insufficient information on the fertiliser management at the experimental plots but also by, for instance, a too high allocation to

grains compared to other tissues. Moreover, under elevated [$CO_2$] a relative increase in root biomass (Pritchard and Rogers, 2000) often occurs. Currently, as discussed in the previous section, there are no explicit mechanisms implemented that would yield such a dynamic growth response. A step forward, that remains to be tested, would be to set a flexible root:shoot allocation via a modification of $f_1$ in response to water or N stress, see Sect. 2.1.1, which would result in such a response in situations when additional leaf C mass in response to elevated [$CO_2$] induced a N demand that cannot be met by soil uptake.

Moreover, as mentioned in Sect. 5.1, SLA in the model is treated as a constant, even though it has been observed to vary over the growing-season, and in response to elevated [$CO_2$] (Poorter et al., 2009). Ainsworth and Long (2005) found in a review of $CO_2$ effects on different plant traits that elevated [$CO_2$] was associated with a reduction in SLA, as the increase in leaf mass was not accompanied by a proportional increase in leaf area. These results are in line with the observed increases in leaf C : N under elevated $CO_2$ (Yin, 2002). Currently in the model the lower limit of leaf N ($N_b$) is a function of SLA (Eq. 9), and whether or not variable SLA would help to constrain the C : N response at variable N and $CO_2$ treatment remains to be tested. While some studies have found elevated $CO_2$ to also change the chemical composition of the plants and thus the C : N (Yin, 2002), others (e.g., Gifford et al., 2000) found no evidence of changes in the C : N of the senesced leaves grown under higher [$CO_2$] implying that the fixed C : N limits and in turn the $N_b$ are valid also under elevated [$CO_2$], but this remains to be explored.

### 5.3 Regional yields, model performance and implications for large scale modelling

The implementation of C–N dynamics improved the ability of LPJ-GUESS to simulate yields not only at local scale but also across larger regions, especially when all permutations of N managements were combined (Fig. 7). As expected, the comparison of the simulated yields with reported ones was best captured when considering time-averaged values (accounting only for the spatial variation) compared to the full temporal variability (difference between "mean" and "all" in Table 5). The discrepancy between results from the C–N and the C-only versions of the model was striking and clearly demonstrates the need to consider

C–N interactions when modelling crop processes (Rosenzweig et al., 2014). In addition to the improved phenology and C–N coupling, which was seen also at the FACE site, on the regional scale the representation of soil texture proved to be an additional important aspect. By incorporating the WISE map of soil mineral fractions, we were able to increase the model performance from a $W_i$ of 0.715 using the standard soil map in LPJ-GUESS simulations with fixed mineral fractions (Smith et al., 2014), to 0.807. With the more detailed soil information, the heterogeneity in the growth response from fertiliser applications due to differences in physical properties could be better captured.

Still, when applied across large spatial domains, there can be multiple reasons for a disagreement between modelled and observed variability that go beyond process representation linked to the basic physiology of C–N interactions. For instance, extreme heat or freezing, pests, or water logging of soils are frequent events detrimental for crop production (Reichstein et al., 2013). Effects of extreme weather events are difficult to account for, partially because of the smoothing effect of a daily time step, and also because aggregation averaging in the production of the gridded climate input data tends to remove weather extremes. Likewise, local management decisions that are not based on weather variability, and their effects on crops and environment, are difficult to capture with the current setup.

Several approaches to modelling N limitations in agricultural ecosystems over large region scales are available in the literature. CLM (Drewniak et al., 2013), e.g. includes N limitation for crops, and this model also simulates the retranslocation of N during the grainfilling period based on prescribed C : N of the plant organs pre- and post anthesis. The C allocation scheme implemented in CLM has the same origin (Penning de Vries et al., 1989) as the one implemented here for LPJ-GUESS. In LPJmL (Fader et al., 2010), an implicit nutrient limitation on yields is considered by varying production parameters ($LAI_{max}$, HI, and $\alpha_a$) to match country or region statistics from e.g. FAO (United Nations Food and Agriculture Organisation). This approach has the advantage that it can be applied without knowledge as to the management (fertilisation) practices that are common in a region, but lacks the possibility to assess effects of future changes in e.g. N fertiliser availability and

changes in management. The crop model GEPIC (Liu et al., 2007) – like LPJmL (Bondeau et al., 2007) – has $LAI_{max}$ and HI as input parameters but also includes N dynamics with empirical response functions as modifiers of productivity and yields. In contrast to LPJmL, GEPIC is based on a site-scale model approach which can be extended in space via a GIS interface that facilitates input of spatially explicit management, where available. WOFOST, a detailed crop-growth model that has recently been expanded to work at larger regions (Boogaard et al., 2013) has demonstrated skills in simulating local and regional yields with a mechanistic approach to modelling crop photosynthesis as well as physiology, but the model approach assumes a continuation of current management practices, and thus cannot be applied for future simulations.

LPJ-GUESS shares several aspects of the approaches of these models: the sowing algorithm (LPJmL Waha et al., 2011), temperature limits for different CFTs (GEPIC), and a large portion of the mechanistic formulations of crop physiology (WOFOST and GECROS are "School of de Wit" models, van Ittersum et al., 2003). Because of the dynamic PHU calculations (Lindeskog et al., 2013) and dynamic sowing and harvest calculations (Waha et al., 2011), LPJ-GUESS can be applied to all areas where suitable temperature and soil moisture conditions allow wheat growth. In addition, we have shown here also that it is possible to find a suitable timing of N fertilisation on the regional-scale by relating the N application to those stages in the crop growing period when it is most needed. For globally applicable models this is an important result, since information on fertiliser application often includes total amounts per year, but typically lacks information about the seasonal distribution.

## 6 Conclusions

The approach chosen here to implement C–N dynamics in the crop module of LPJ-GUESS seeks to adopt mechanistic process implementations, which has been advocated in literature to be able to fully capture the effects of climate change on ecosystems. The modelling framework demonstrably responds realistically to different N fertiliser treatments

and [$CO_2$] and produces results that are in line with observations from site-scale to a larger region.

These findings support the aim of this study, to find a level of complexity in the implementation of the N management that can be applied on larger regions, and that is ultimately also applicable under climate and other environmental changes. As long as spatially estimated total N applications are available, adopting mean treatment of timing of the N in the model that is based on the development stage appears sufficient for representing the mean and variance of regional yields.

Representing dynamic C–N interactions within a consistent terrestrial modelling framework provides the capacity to predict changes in global C and N pools and fluxes in historic or future land-use change scenarios, as well as to quantify and explore the effect of different managements on the global C and N budgets, considering hindcasts and projections of land-use change (e.g. Hurtt et al., 2011; Klein Goldewijk et al., 2011), climate change and historic or future N fertiliser application rates (e.g. Potter et al., 2010; Bouwman et al., 2013).

## Appendix A

*Acknowledgements.* This study is a contribution to the Strong Research Environment Land-Use Today and Tomorrow funded by the Swedish Research Council FORMAS (Contract No. 211-2009-1682). Almut Arneth and Per Bodin acknowledge support from the EU-FP7 project ClimAfrica (244240). Almut Arneth acknowledges support from EU-FP7 projects LUC4C (603542) and EMBRACE (282672). Guy Schurgers and Jennie Holmér acknowledge support from the Strategic Research Area BECC. Mats Lindeskog was funded by the Mistra Swedish Research Programme for Climate, Impacts and Adaptation. This study is a contribution to the Strategic Research Areas BECC and MERGE and to the Lund University Centre for Studies of Carbon Cycle and Climate Interactions (LUCCI).

## References


Ainsworth, E. A. and Long, S. P.: What have we learned from 15 years of free-air $CO_2$ enrichment (FACE)? A meta-analytic review of the responses of photosynthesis, canopy properties and plant production to rising $CO_2$, New Phytol., 165, 351–372, doi:10.1111/j.1469-8137.2004.01224.x, 2005.

Ainsworth, E. A. and Rogers, A.: The response of photosynthesis and stomatal conductance to rising [$CO_2$]: mechanisms and environmental interactions, Plant Cell Environ., 30, 258–270, doi:10.1111/j.1365-3040.2007.01641.x, 2007.

Ainsworth, E. A., Leakey, A. D. B., Ort, D. R., and Long, S. P.: FACE-ing the facts: inconsistencies and interdependence among field, chamber and modeling studies of elevated [$CO_2$] impacts on crop yield and food supply, New Phytol., 179, 5–9, doi:10.1111/j.1469-8137.2008.02500.x, 2008.

Anten, N., Schieving, F., and Werger, M.: Patterns of light and nitrogen distribution in relation to whole canopy carbon gain in C3 and C4 mono- and dicotyledonous species, Oecologia, 101, 504–513, doi:10.1007/BF00329431, 1995.

Arneth, A., Sitch, S., Bondeau, A., Butterbach-Bahl, K., Foster, P., Gedney, N., de Noblet-Ducoudré, N., Prentice, I. C., Sanderson, M., Thonicke, K., Wania, R., and Zaehle, S.: From biota to chemistry and climate: towards a comprehensive description of trace gas exchange between the biosphere and atmosphere, Biogeosciences, 7, 121–149, doi:10.5194/bg-7-121-2010, 2010.

Arora, V. K.: Simulating energy and carbon fluxes over winter wheat using coupled land surface and terrestrial ecosystem models, Agr. Forest Meteorol., 118, 21–47, doi:10.1016/S0168-1923(03)00073-X, 2003.

Asseng, S., Jamieson, P., Kimball, B., Pinter, P., Sayre, K., Bowden, J., and Howden, S.: Simulated wheat growth affected by rising temperature, increased water deficit and elevated atmospheric $CO_2$, Field Crop. Res., 85, 85–102, doi:10.1016/S0378-4290(03)00154-0, 2004.

Ayres, R. U., Schlesinger, W. H., and Socolow, R. H.: Human impacts on the carbon and nitrogen cycles, Industrial Ecology and Global Change, Cambridge University Press, Cambridge, UK, 121–155, 1994.

Batjes, N. H.: ISRICE-WISE global data ser of derived soil properties on a 0.5 by 0.5 degree grid (version 3.0), Report 08, ISRIC – World Soil Information, Wageningen, 2005.

Bertheloot, J., Martre, P., and Andrieu, B.: Dynamics of Light and Nitrogen Distribution during Grain Filling within Wheat Canopy, Plant Physiol., 148, 1707–1720, doi:10.1104/pp.108.124156, 2008.

Bondeau, A., Smith, P. C., Zaehle, S., Schaphoff, S., Lucht, W., Cramer, W., and Gerten, D.: Modelling the role of agriculture for the 20th century global terrestrial carbon balance, Glob. Change Biol., 13, 679–706, 2007.

Boogaard, H., Wolf, J., Supit, I., Niemeyer, S., and van Ittersum, M.: A regional implementation of WOFOST for calculating yield gaps of autumn-sown wheat across the European Union, Crop Yield Gap Analysis – Rationale, Methods and Applications, Field Crop. Res., 143, 130–142, doi:10.1016/j.fcr.2012.11.005, 2013.

Boote, K. J., Jones, J. W., White, J. W., Asseng, S., and Lizaso, J. I.: Putting mechanisms into crop production models, Plant Cell Environ., 36, 1658–1672, doi:10.1111/pce.12119, 2013.

Bouwman, L., Goldewijk, K. K., Van Der Hoek, K. W., Beusen, A. H. W., Van Vuuren, D. P., Willems, J., Rufino, M. C., and Stehfest, E.: Exploring global changes in nitrogen and phosphorus cycles in agriculture induced by livestock production over the 1900–2050 period, P. Natl. Acad. Sci. USA, 110, 20882–20887, doi:10.1073/pnas.1012878108, 2013.

Cosby, B. J., Hornberger, G. M., Clapp, R. B., and Ginn, T. R.: A Statistical Exploration of the Relationships of Soil Moisture Characteristics to the Physical Properties of Soils, Water Resour. Res., 20, 682–690, doi:10.1029/WR020i006p00682, 1984.

Dee, D. P., Uppala, S. M., Simmons, A. J., Berrisford, P., Poli, P., Kobayashi, S., Andrae, U., Balmaseda, M. A., Balsamo, G., Bauer, P., Bechtold, P., Beljaars, A. C. M., van de Berg, L., Bidlot, J., Bormann, N., Delsol, C., Dragani, R., Fuentes, M., Geer, A. J., Haimberger, L., Healy, S. B., Hersbach, H., Hólm, E. V., Isaksen, L., Kållberg, P., Köhler, M., Matricardi, M., McNally, A. P., Monge-Sanz, B. M., Morcrette, J.-J., Park, B.-K., Peubey, C., de Rosnay, P., Tavolato, C., Thépaut, J.-N., and Vitart, F.: The ERA-Interim reanalysis: configuration and performance of the data assimilation system, Q. J. Roy. Meteor. Soc., 137, 553–597, doi:10.1002/qj.828, 2011.

Deryng, D., Sacks, W. J., Barford, C. C., and Ramankutty, N.: Simulating the effects of climate and agricultural management practices on global crop yield, Global Biogeochem. Cy., 25, GB2006, doi:10.1029/2009GB003765, 2011.

Drake, B. G., Gonzalez-Meler, M. A., and Long, S. P.: More efficient plants: a consequence of rising atmospheric $CO_2$?, Annu. Rev. Plant Phys., 48, 609–639, doi:10.1146/annurev.arplant.48.1.609, 1997.

Drewniak, B., Song, J., Prell, J., Kotamarthi, V. R., and Jacob, R.: Modeling agriculture in the Community Land Model, Geosci. Model Dev., 6, 495–515, doi:10.5194/gmd-6-495-2013, 2013.

Elliott, J., Müller, C., Deryng, D., Chryssanthacopoulos, J., Boote, K. J., Büchner, M., Foster, I., Glotter, M., Heinke, J., Iizumi, T., Izaurralde, R. C., Mueller, N. D., Ray, D. K., Rosenzweig, C., Ruane, A. C., and Sheffield, J.: The Global Gridded Crop Model intercomparison: data and modeling protocols for Phase 1 (v1.0), Geosci. Model Dev. Discuss., 7, 4383–4427, doi:10.5194/gmdd-7-4383-2014, 2014.

Evans, J. R.: Photosynthesis and nitrogen relationships in leaves of C3 plants, Oecologia, 78, 9–19, doi:10.1007/BF00377192, 1989a.

Evans, J. R.: Partitioning of Nitrogen Between and Within Leaves Grown Under Different Irradiances, Functional Plant Biol., 16, 533–548, doi:10.1071/PP9890533, 1989b.

Fader, M., Rost, S., Muller, C., Bondeau, A., and Gerten, D.: Virtual water content of temperate cereals and maize: Present and potential future patterns, J. Hydrol., 384, 218–231, 2010.

Fischer, G., Shah, M., van Velthuizen, H., and Nachtergaele, F. O.: Global agro-ecological assessment for agriculture in the 21st century, Research Report RR-02-02, 2001.

Friedlingstein, P., Meinshausen, M., Arora, V. K., Jones, C. D., Anav, A., Liddicoat, S. K., and Knutti, R.: Uncertainties in CMIP5 climate projections due to carbon cycle feedbacks, J. Climate, 27, 511–526, doi:10.1175/JCLI-D-12-00579.1, 2013.

Galloway, J. N., Dentener, F. J., Capone, D. G., Boyer, E. W., Howarth, R. W., Seitzinger, S. P., Asner, G. P., Cleveland, C. C., Green, P. A., Holland, E. A., Karl, D. M., Michaels, A. F., Porter, J. H., Townsend, A. R., and Vörösmarty, C. J.: Nitrogen cycles: past, present, and future, Biogeochemistry, 70, 153–226, doi:10.1007/s10533-004-0370-0, 2004.

Gerten, D., Schaphoff, S., Haberlandt, U., Lucht, W., and Sitch, S.: Terrestrial vegetation and water balance – hydrological evaluation of a dynamic global vegetation model, J. Hydrol., 286, 249–270, doi:10.1016/j.jhydrol.2003.09.029, 2004.

Gifford, R., Barrett, D., and Lutze, J.: The effects of elevated [$CO_2$] on the C : N and C : P mass ratios of plant tissues, Plant Soil, 224, 1–14, doi:10.1023/A:1004790612630, 2000.

Grindlay, D. J. C.: REVIEW Towards an explanation of crop nitrogen demand based on the optimization of leaf nitrogen per unit leaf area, J. Agr. Sci., 128, 377–396, http://journals.cambridge.org/article_S0021859697004310, 1997.

Groot, J. and Verberne, E.: Response of wheat to nitrogen fertilization, a data set to validate simulation models for nitrogen dynamics in crop and soil, Fert. Res., 27, 349–383, doi:10.1007/BF01051140, 1991.

Gruber, N. and Galloway, J. N.: An Earth-system perspective of the global nitrogen cycle, Nature, 451, 293–296, 2008.

Hawkesford, M. J.: Reducing the reliance on nitrogen fertilizer for wheat production, Cereal Science for Food Security,Nutrition and Sustainability, J. Cereal Sci., 59, 276–283, doi:10.1016/j.jcs.2013.12.001, 2014.

Haxeltine, A. and Prentice, I. C.: A general model for the light-use efficiency of primary production, Funct. Ecol., 10, 551–561, 1996a.

Haxeltine, A. and Prentice, I. C.: BIOME3: an equilibrium terrestrial biosphere model based on ecophysiological constraints, resource availability, and competition among plant functional types, Global Biogeochem. Cy., 10, 693–709, doi:10.1029/96GB02344, 1996b.

Hickler, T., Smith, B., Sykes, M. T., Davis, M. B., Sugita, S., and Walker, K.: Using a generalized vegetation model to simulate vegetation dynamics in Northeastern USA, Ecology, 85, 519–530, doi:10.1890/02-0344, 2004.

Hirose, T.: Development of the Monsi–Saeki Theory on canopy structure and function, Ann. Bot.-London, 95, 483–494, doi:10.1093/aob/mci047, 2005.

Hirose, T. and Werger, M.: Maximizing daily canopy photosynthesis with respect to the leaf nitrogen allocation pattern in the canopy, Oecologia, 72, 520–526, doi:10.1007/BF00378977, 1987.

Hollinger, D. Y.: Optimality and nitrogen allocation in a tree canopy, Tree Physiol., 16, 627–634, doi:10.1093/treephys/16.7.627, 1996.

Hurtt, G., Chini, L., Frolking, S., Betts, R., Feddema, J., Fischer, G., Fisk, J., Hibbard, K., Houghton, R., Janetos, A., Jones, C., Kindermann, G., Kinoshita, T., Klein Goldewijk, K., Riahi, K., Shevliakova, E., Smith, S., Stehfest, E., Thomson, A., Thornton, P., van Vuuren, D., and Wang, Y.: Harmonization of land-use scenarios for the period 1500–2100: 600 years of global gridded annual land-use transitions, wood harvest, and resulting secondary lands, Climatic Change, 109, 117–161, doi:10.1007/s10584-011-0153-2, 2011.

Kelley, D. I., Prentice, I. C., Harrison, S. P., Wang, H., Simard, M., Fisher, J. B., and Willis, K. O.: A comprehensive benchmarking system for evaluating global vegetation models, Biogeosciences, 10, 3313–3340, doi:10.5194/bg-10-3313-2013, 2013.

Klein Goldewijk, K., Beusen, A., van Drecht, G., and de Vos, M.: The HYDE 3.1 spatially explicit database of human-induced global land-use change over the past 12 000 years, Global Ecol. Biogeogr., 20, 73–86, doi:10.1111/j.1466-8238.2010.00587.x, 2011.

Kull, O.: Acclimation of photosynthesis in canopies: models and limitations, Oecologia, 133, 267–279, doi:10.1007/s00442-002-1042-1, 2002.

Kull, O. and Jarvis, P.: The role of Nitrogen in a simple scheme to scale-up photosynthesis from leaf to canopy, Plant Cell Environ., 18, 1174–1182, doi:10.1111/j.1365-3040.1995.tb00627.x, 1995.

Kunkle, J. M., Walters, M. B., and Kobe, R. K.: Senescence-related changes in nitrogen in fine roots: mass loss affects estimation, Tree Physiol., 29, 715–723, doi:10.1093/treephys/tpp004, 2009.

Lamarque, J.-F., Bond, T. C., Eyring, V., Granier, C., Heil, A., Klimont, Z., Lee, D., Liousse, C., Mieville, A., Owen, B., Schultz, M. G., Shindell, D., Smith, S. J., Stehfest, E., Van Aardenne, J., Cooper, O. R., Kainuma, M., Mahowald, N., McConnell, J. R., Naik, V., Riahi, K., and van Vuuren, D. P.: Historical (1850–2000) gridded anthropogenic and biomass burning emissions of reactive gases and aerosols: methodology and application, Atmos. Chem. Phys., 10, 7017–7039, doi:10.5194/acp-10-7017-2010, 2010.

Levis, S., Bonan, G. B., Kluzek, E., Thornton, P. E., Jones, A., Sacks, W. J., and Kucharik, C. J.: Interactive Crop Management in the Community Earth System Model (CESM1): seasonal influences on land–atmosphere fluxes, J. Climate, 25, 4839–4859, doi:10.1175/JCLI-D-11-00446.1, 2012.

Lindeskog, M., Arneth, A., Bondeau, A., Waha, K., Seaquist, J., Olin, S., and Smith, B.: Implications of accounting for land use in simulations of ecosystem carbon cycling in Africa, Earth Syst. Dynam., 4, 385–407, doi:10.5194/esd-4-385-2013, 2013.

Liu, J., Williams, J. R., Zehnder, A. J., and Yang, H.: GEPIC – modelling wheat yield and crop water productivity with high resolution on a global scale, Agr. Syst., 94, 478–493, doi:10.1016/j.agsy.2006.11.019, 2007.

Lobell, D. B., Banziger, M., Magorokosho, C., and Vivek, B.: Nonlinear heat effects on African maize as evidenced by historical yield trials, Nature Climate Change, 1, 42–45, doi:10.1038/nclimate1043, 2011.

Lokupitiya, E., Denning, S., Paustian, K., Baker, I., Schaefer, K., Verma, S., Meyers, T., Bernacchi, C. J., Suyker, A., and Fischer, M.: Incorporation of crop phenology in Simple Biosphere Model (SiBcrop) to improve land-atmosphere carbon exchanges from croplands, Biogeosciences, 6, 969–986, doi:10.5194/bg-6-969-2009, 2009.

Long, S. P.: Modification of the response of photosynthetic productivity to rising temperature by atmospheric $CO_2$ concentrations: Has its importance been underestimated?, Plant Cell Environ., 14, 729–739, doi:10.1111/j.1365-3040.1991.tb01439.x, 1991.

Mahler, R. L., Koehler, F. E., and Lutcher, L. K.: Nitrogen Source, Timing of Application, and Placement: Effects on Winter Wheat Production, Agron. J., 637–642, doi:10.2134/agronj1994.00021962008600040010x 1994.

Masclaux-Daubresse, C., Daniel-Vedele, F., Dechorgnat, J., Chardon, F., Gaufichon, L., and Suzuki, A.: Nitrogen uptake, assimilation and remobilization in plants: challenges for sustainable and productive agriculture, Ann. Bot.-London, 105, 1141–1157, doi:10.1093/aob/mcq028, 2010.

McGuire, A. D., Sitch, S., Clein, J. S., Dargaville, R., Esser, G., Foley, J., Heimann, M., Joos, F., Kaplan, J., Kicklighter, D. W., Meier, R. A., Melillo, J. M., Moore, B., Prentice, I. C., Ramankutty, N., Reichenau, T., Schloss, A., Tian, H., Williams, L. J., and Wittenberg, U.: Carbon balance of the terrestrial biosphere in the twentieth century: analyses of $CO_2$, climate and land use effects with four process-based ecosystem models, Global Biogeochem. Cy., 15, 183–206, doi:10.1029/2000GB001298, 2001.

Olesen, J., Trnka, M., Kersebaum, K., Skjelvåg, A., Seguin, B., Peltonen-Sainio, P., Rossi, F., Kozyra, J., and Micale, F.: Impacts and adaptation of European crop production systems to climate change, Eur. J. Agron., 34, 96–112, doi:10.1016/j.eja.2010.11.003, 2011.

Osaki, M., Shinano, T., and Tadano, T.: Redistribution of carbon and nitrogen compounds from the shoot to the harvesting organs during maturation in field crops, Soil Sci. Plant Nutr., 37, 117–128, doi:10.1080/00380768.1991.10415017, 1991.

Osaki, M., Shinano, T., and Tadano, T.: Carbon-nitrogen interaction in field crop production, Soil Sci. Plant Nutr., 38, 553–564, 1992.

Parton, W. J., Scurlock, J. M. O., Ojima, D. S., Gilmanov, T. G., Scholes, R. J., Schimel, D. S., Kirchner, T., Menaut, J.-C., Seastedt, T., Garcia Moya, E., Kamnalrut, A., and Kinyamario, J. I.: Observations and modeling of biomass and soil organic matter dynamics for the grassland biome worldwide, Global Biogeochem. Cy., 7, 785–809, doi:10.1029/93GB02042, 1993.

Penning de Vries, F. W. T., Jansen, D. M., Berge, H. F. M., and Bakema, A.: Simulation of ecophysiological processes of growth in several annual crops., Centre for Agricultural Publishing and Documentation, Wageningen, the Netherlands, 1989.

Poorter, H., Niinemets, U., Poorter, L., Wright, I. J., and Villar, R.: Causes and consequences of variation in leaf mass per area (LMA): a meta-analysis, New Phytol., 182, 565–588, doi:10.1111/j.1469-8137.2009.02830.x, 2009.

Poorter, H., Niklas, K. J., Reich, P. B., Oleksyn, J., Poot, P., and Mommer, L.: Biomass allocation to leaves, stems and roots: meta-analyses of interspecific variation and environmental control, New Phytol., 193, 30–50, doi:10.1111/j.1469-8137.2011.03952.x, 2012.

Portmann, F. T., Siebert, S., and Döll, P.: MIRCA2000–Global monthly irrigated and rainfed crop areas around the year 2000: A new high-resolution data set for agricultural and hydrological modeling, Global Biogeochem. Cy., 24, GB1011, doi:10.1029/2008GB003435, 2010.

Potter, P., Ramankutty, N., Bennett, E. M., and Donner, S. D.: Characterizing the Spatial Patterns of Global Fertilizer Application and Manure Production, Earth Interact., 14, 1–22, doi:10.1175/2009EI288.1, 2010.

Prentice, I., Bondeau, A., Cramer, W., Harrison, S., Hickler, T., Lucht, W., Sitch, S., Smith, B., and Sykes, M.: Dynamic Global Vegetation Modeling: Quantifying Terrestrial Ecosystem Responses to Large-Scale Environmental Change, in: Terrestrial Ecosystems in a Changing World, edited by Canadell, J., Pataki, D., and Pitelka, L., Global Change – The IGBP Series, Springer, Berlin Heidelberg, 175–192, doi:10.1007/978-3-540-32730-1_15, 2007.

Pritchard, S. G. and Rogers, H. H.: Spatial and temporal deployment of crop roots in $CO_2$-enriched environments, New Phytol., 147, 55–71, doi:10.1046/j.1469-8137.2000.00678.x, 2000.

Reichstein, M., Bahn, M., Ciais, P., Frank, D., Mahecha, M. D., Seneviratne, S. I., Zscheischler, J., Beer, C., Buchmann, N., Frank, D. C., Papale, D., Rammig, A., Smith, P., Thonicke, K., van der Velde, M., Vicca, S., Walz, A., and Wattenbach, M.: Climate extremes and the carbon cycle, Nature, 500, 287–295, doi:10.1038/nature12350, 2013.

Richards, F. J.: A Flexible Growth Function for Empirical Use, J. Exp. Bot., 10, 290–301, doi:10.1093/jxb/10.2.290, 1959.

Rockstrom, J., Steffen, W., Noone, K., Persson, A., Chapin, F. S., Lambin, E. F., Lenton, T. M., Scheffer, M., Folke, C., Schellnhuber, H. J., Nykvist, B., de Wit, C. A., Hughes, T., van der Leeuw, S., Rodhe, H., Sorlin, S., Snyder, P. K., Costanza, R., Svedin, U., Falkenmark, M., Karlberg, L., Corell, R. W., Fabry, V. J., Hansen, J., Walker, B., Liverman, D., Richardson, K., Crutzen, P., and Foley, J. A.: A safe operating space for humanity, Nature, 461, 472–475, doi:10.1038/461472a, 2009.

Rosenzweig, C. and Tubiello, F.: Adaptation and mitigation strategies in agriculture: an analysis of potential synergies, Mitigation and Adaptation Strategies for Global Change, 12, 855–873, doi:10.1007/s11027-007-9103-8, 2007.

Rosenzweig, C., Elliott, J., Deryng, D., Ruane, A. C., Müller, C., Arneth, A., Boote, K. J., Folberth, C., Glotter, M., Khabarov, N., Neumann, K., Piontek, F., Pugh, T. A. M., Schmid, E., Stehfest, E., Yang, H., and Jones, J. W.: Assessing agricultural risks of climate change in the 21st century in a global gridded crop model intercomparison, P. Natl. Acad. Sci. USA, doi:10.1073/pnas.1222463110, 2014.

Rounsevell, M. D. A., Arneth, A., Alexander, P., Brown, D. G., de Noblet-Ducoudré, N., Ellis, E., Finnigan, J., Galvin, K., Grigg, N., Harman, I., Lennox, J., Magliocca, N., Parker, D., O'Neill, B. C., Verburg, P. H., and Young, O.: Towards decision-based global land use models for improved

understanding of the Earth system, Earth Syst. Dynam., 5, 117–137, doi:10.5194/esd-5-117-2014, 2014.

Schlenker, W. and Roberts, M. J.: Nonlinear temperature effects indicate severe damages to U. S. crop yields under climate change, P. Natl. Acad. Sci. USA, 106, 15594–15598, doi:10.1073/pnas.0906865106, 2009.

Seligman, N., Keulen, H., and Goudriaan, J.: An elementary model of nitrogen uptake and redistribution by annual plant species, Oecologia, 21, 243–261, doi:10.1007/PL00020264, 1975.

Shevliakova, E., Stouffer, R. J., Malyshev, S., Krasting, J. P., Hurtt, G. C., and Pacala, S. W.: Historical warming reduced due to enhanced land carbon uptake, P. Natl. Acad. Sci. USA, doi:10.1073/pnas.1314047110, 2013.

Sinclair, T. and Amir, J.: A model to assess nitrogen limitations on the growth and yield of spring wheat, Field Crop. Res., 30, 63–78, doi:10.1016/0378-4290(92)90057-G, 1992.

Sitch, S., Smith, B., Prentice, I. C., Arneth, A., Bondeau, A., Cramer, W., Kaplan, J. O., Levis, S., Lucht, W., Sykes, M. T., Thonicke, K., and Venevsky, S.: Evaluation of ecosystem dynamics, plant geography and terrestrial carbon cycling in the LPJ dynamic global vegetation model, Glob. Change Biol., 9, 161–185, doi:10.1046/j.1365-2486.2003.00569.x, 2003.

Smith, B., Prentice, I. C., and Sykes, M. T.: Representation of vegetation dynamics in the modelling of terrestrial ecosystems: comparing two contrasting approaches within European climate space, Global Ecol. Biogeogr., 10, 621–637, 2001.

Smith, B., Wårlind, D., Arneth, A., Hickler, T., Leadley, P., Siltberg, J., and Zaehle, S.: Implications of incorporating N cycling and N limitations on primary production in an individual-based dynamic vegetation model, Biogeosciences, 11, 2027–2054, doi:10.5194/bg-11-2027-2014, 2014.

Smith, N. G. and Dukes, J. S.: Plant respiration and photosynthesis in global-scale models: incorporating acclimation to temperature and $CO_2$, Glob. Change Biol., 19, 45–63, doi:10.1111/j.1365-2486.2012.02797.x, 2013.

Stehfest, E., Heistermann, M., Priess, J. A., Ojima, D. S., and Alcamo, J.: Simulation of global crop production with the ecosystem model DayCent, Ecol. Model., 209, 203–219, doi:10.1016/j.ecolmodel.2007.06.028, 2007.

Sun, Y., Gu, L., Dickinson, R. E., Norby, R. J., Pallardy, S. G., and Hoffman, F. M.: Impact of mesophyll diffusion on estimated global land $CO_2$ fertilization, P. Natl. Acad. Sci. USA, doi:10.1073/pnas.1418075111, 2014.

Thomas, H. and Stoddart, J. L.: Leaf Senescence, Ann. Revi. Plant Physiol., 31, 83–111, doi:10.1146/annurev.pp.31.060180.000503, 1980.

Thornley, J.: Plant and Crop Modelling: A Mathematical Approach to Plant and Crop Physiology, Clarendon Press, Oxford, 1990.

Thornton, P., Law, B., Gholz, H. L., Clark, K. L., Falge, E., Ellsworth, D., Goldstein, A., Monson, R., Hollinger, D., Falk, M., Chen, J., and Sparks, J.: Modeling and measuring the effects of disturbance history and climate on carbon and water budgets in evergreen needleleaf forests, Agr. Forest Meteorol., 113, 185–222, doi:10.1016/S0168-1923(02)00108-9, {FLUXNET} 2000 Synthesis, 2002.

Thornton, P. E., Doney, S. C., Lindsay, K., Moore, J. K., Mahowald, N., Randerson, J. T., Fung, I., Lamarque, J.-F., Feddema, J. J., and Lee, Y.-H.: Carbon-nitrogen interactions regulate climate-carbon cycle feedbacks: results from an atmosphere-ocean general circulation model, Biogeosciences, 6, 2099–2120, doi:10.5194/bg-6-2099-2009, 2009.

Tilman, D., Fargione, J., Wolff, B., D'Antonio, C., Dobson, A., Howarth, R., Schindler, D., Schlesinger, W. H., Simberloff, D., and Swackhamer, D.: Forecasting agriculturally driven global environmental change, Science, 292, 281–284, doi:10.1126/science.1057544, 2001.

Tilman, D., Cassman, K. G., Matson, P. A., Naylor, R., and Polasky, S.: Agricultural sustainability and intensive production practices, Nature, 418, 671–677, doi:10.1038/nature01014, 2002.

Tubiello, F. N. and Ewert, F.: Simulating the effects of elevated $CO_2$ on crops: approaches and applications for climate change, Process simulation and application of cropping system models, Eur. J. Agron., 18, 57–74, doi:10.1016/S1161-0301(02)00097-7, 2002.

van Ittersum, M., Leffelaar, P., van Keulen, H., Kropff, M., Bastiaans, L., and Goudriaan, J.: On approaches and applications of the Wageningen crop models, Modelling cropping systems: science, software and applications, Eur. J. Agron., 18, 201–234, doi:10.1016/S1161-0301(02)00106-5, 2003.

van Keulen, H., J. G., and Seligman, N.: Plant canopies: their growth, form and function: modelling the effects of nitrogen on canopy development and crop growth, Cambridge University Press, Cambridge, UK, 83–104, doi:10.1017/CBO9780511752308.006, 1989.

Vitousek, P. M., Mooney, H. A., Lubchenco, J., and Melillo, J. M.: Human domination of Earth's ecosystems, Science, 277, 494–499, doi:10.1126/science.277.5325.494, 1997.

Vitousek, P. M., Cassman, K., Cleveland, C., Crews, T., Field, C. B., Grimm, N. B., Howarth, R. W., Marino, R., Martinelli, L., Rastetter, E. B., and Sprent, J. I.: Towards an ecological understanding of biological nitrogen fixation, Biogeochemistry, 57–58, 1–45, doi:10.1023/A:1015798428743, 2002.

Waha, K., van Bussel, L. G. J., Muller, C., and Bondeau, A.: Climate-driven simulation of global crop sowing dates, Global Ecol. Biogeogr., doi:10.1111/j.1466-8238.2011.00678.x, 2011.

Wang, E. and Engel, T.: Simulation of phenological development of wheat crops, Agr. Syst., 58, 1–24, doi:10.1016/S0308-521X(98)00028-6, 1998.

Wårlind, D., Smith, B., Hickler, T., and Arneth, A.: Nitrogen feedbacks increase future terrestrial ecosystem carbon uptake in an individual-based dynamic vegetation model, Biogeosciences, 11, 6131–6146, doi:10.5194/bg-11-6131-2014, 2014.

Weedon, G. P., Gomes, S., Viterbo, P., Shuttleworth, W. J., Blyth, E., Österle, H., Adam, J. C., Bellouin, N., Boucher, O., and Best, M.: Creation of the WATCH forcing data and its use to assess global and regional reference crop evaporation over land during the twentieth century, J. Hydrometeorol., 12, 823–848, doi:10.1175/2011JHM1369.1, 2011.

Weedon, G. P., Gomes, S., Balsamo, G., Best, M. J., Bellouin, N., and Viterbo, P.: WATCH forcing data based on ERA-INTERIM, available at: ftp://rfdata:forceDATA@ftp.iiasa.ac.at (last access: 20 June 2014), 2012.

Weigel, H.-J. and Manderscheid, R.: Crop growth responses to free air $CO_2$ enrichment and nitrogen fertilization: rotating barley, ryegrass, sugar beet and wheat, Eur. J. Agron., 43, 97–107, doi:10.1016/j.eja.2012.05.011, 2012.

Willmott, C. J., Robeson, S. M., and Matsuura, K.: A refined index of model performance, Int. J. Climatol., 32, 2088–2094, doi:10.1002/joc.2419, 2012.

Xu-Ri and Prentice, I. C.: Terrestrial nitrogen cycle simulation with a dynamic global vegetation model, Glob. Change Biol., 14, 1745–1764, doi:10.1111/j.1365-2486.2008.01625.x, 2008.

Yin, X.: Responses of leaf nitrogen concentration and specific leaf area to atmospheric $CO_2$ enrichment: a retrospective synthesis across 62 species, Glob. Change Biol., 8, 631–642, doi:10.1046/j.1365-2486.2002.00497.x, 2002.

Yin, X.: Improving ecophysiological simulation models to predict the impact of elevated atmospheric $CO_2$ concentration on crop productivity, Ann. Bot.-London, 112, 465–475, doi:10.1093/aob/mct016, 2013.

Yin, X. and Struik, P. C.: Modelling the crop: from system dynamics to systems biology, J. Exp. Bot., 61, 2171–2183, doi:10.1093/jxb/erp375, 2010.

Yin, X. and Van Laar, H.: Crop systems dynamics: an ecophysiological simulation model for genotype-by-environment interactions, Wageningen Academic Pub.,Wageningen, the Netherlands, 2005.

Yin, X., Schapendonk, A. H. C. M., Kropff, M. J., van Oijen, M., and Bindraban, P. S.: A generic equation for nitrogen-limited leaf area index and its application in crop growth models for predicting leaf senescence, Ann. Bot.-London, 85, 579–585, doi:10.1006/anbo.1999.1104, 2000.

Yin, X., Lantinga, E. A., Schanendonk, A. H. C. M., and Zhong, X.: Some quantitative relationships between leaf area index and canopy nitrogen content and distribution, Ann. Bot.-London, 91, 893–903, doi:10.1093/aob/mcg096, 2003.

Zaehle, S. and Friend, A. D.: Carbon and nitrogen cycle dynamics in the O-CN land surface model: 1. Model description, site-scale evaluation, and sensitivity to parameter estimates, Global Biogeochem. Cy., 24, GB1005, doi:10.1029/2009GB003521, 2010.

**Table 1.** Site and treatment specific data after Groot and Verberne (1991). For all trials (I–VI), three experiments with different applications of N fertiliser were performed (1,2 and 3). Their timing is expressed here by the development stage (DS).

| Site Location, soil | | Trial | season | DS | N app. ($kg\ N\ ha^{-1}$) 1 | 2 | 3 |
|---|---|---|---|---|---|---|---|
| The Eest, 5.75° E, 52.62° N | | I | 1982–1983 | 0.25 | 0 | 0 | 0 |
| | | | | 0.51 | 0 | 60 | 0 |
| | | | | 1.02 | 0 | 120 | 40 |
| Sand | 0.10 | II | 1983–1984 | 0.04 | 70 | 0 | 0 |
| Silt | 0.55 | | | 0.49 | 70 | 60 | 40 |
| Clay | 0.35 | | | 0.63 | 70 | 120 | 40 |
| The Bouwing, 5.75° E, 52.95° N | | III | 1982–1983 | 0.25 | 0 | 0 | 0 |
| | | | | 0.51 | 0 | 60 | 0 |
| | | | | 1.02 | 0 | 120 | 40 |
| Sand | 0.15 | IV | 1983–1984 | 0.26 | 50 | 60 | 0 |
| Silt | 0.55 | | | 0.49 | 50 | 60 | 40 |
| Clay | 0.30 | | | 0.99 | 50 | 60 | 40 |
| PAGV, 5.5° E, 52.5° N | | V | 1982–1983 | 0.25 | 80 | 0 | 0 |
| | | | | 0.47 | 60 | 80 | 0 |
| | | | | 0.98 | 60 | 140 | 40 |
| Sand | 0.15 | VI | 1983–1984 | 0.08 | 80 | 0 | 0 |
| Silt | 0.55 | | | 0.49 | 80 | 60 | 40 |
| Clay | 0.30 | | | 0.74 | 80 | 120 | 40 |

**Table 2.** Description of the experiments carried at the Braunschweig research station in Germany and how it was modelled in LPJ-GUESS. For a more detailed description of the experiments see Table 1 in Weigel and Manderscheid (2012).

| Management | Units | 1999/2000 Barley* | 2001/2002 Wheat | 2002/2003 Barley* | 2004/2005 Wheat |
|---|---|---|---|---|---|
| Sowing | Date | 24.09.99 | 06.11.01 | 27.09.02 | 26.10.04 |
| N-fert. (H/L) | $kg\,ha^{-1}$ | 262/105 | 251/114 | 179/105 | 168/84 |
| Final harvest | Date | 26.06.00 | 31.07.02 | 25.06.03 | 27.07.05 |
| $[CO_2]$ (amb./elev.) | ppm | 373/549 | 377/548 | 378/547 | 378/549 |

* Modelled as wheat.

**Table 3.** Description of the setups used in the comparison with regional statistics, with abbreviations used throughout the paper.

| Setup | Description | Timing | N app. |
|---|---|---|---|
| $F_{\mathrm{T,A}}$ | 50 permutations, with timing and application rate varied | varied | varied |
| $F_{\mathrm{opt(T,A)}}$ | optimised timing and rate based on model fit (RMSE) in comparison to regional yield statistis | opt. | opt. |
| $F_{\mathrm{t,a}}$ | mean timing and application rate over all regions from $F_{\mathrm{opt(T,A)}}$ | fixed | fixed |
| $F_{\mathrm{T,a}}$ | 10 permutations with timing varied as in $F_{\mathrm{T,A}}$, application rate from $F_{\mathrm{opt(T,A)}}$ | varied | fixed |
| $F_{\mathrm{t,A}}$ | 5 permutations with timing from $F_{\mathrm{opt(T,A)}}$, application rate from $F_{\mathrm{T,A}}$ | fixed | varied |
| $F_{\mathrm{t,I}}$ | Timing from $F_{\mathrm{opt(T,A)}}$, application rate from (Elliott et al., 2014) | fixed | input |
| $F_{\mathrm{C}}$ | C only | | |

**Table 4.** Comparison of modelled and observed grain C : N from a FACE experiment where wheat was grown in ambient $CO_2$ ($\sim$ 378 ppm) and elevated $CO_2$ ($\sim$ 548 ppm). The observed C : N where compiled using Tables 4 and 5 in Weigel and Manderscheid (2012), observed C values where derived from dry matter using the conversion described in Sect. 3.5. The range of the observed $CO_2$ effect is estimated from the standard errors listed in Tables 4 and 5 in Weigel and Manderscheid (2012).

| | | Ambient $CO_2$ | | Elevated $CO_2$ | | $CO_2$ effect (%) | |
|---|---|---|---|---|---|---|---|
| | year | 100 % N | 50 % N | 100 % N | 50 % N | 100 % N | 50 % N |
| Modelled | 2000 | 21.7 | 16.1 | 27.9 | 20.8 | 28 | 29 |
| | 2002 | 21.0 | 17.9 | 24.1 | 21.1 | 15 | 18 |
| | 2003 | 16.1 | 13.5 | 21.5 | 15.1 | 33 | 12 |
| | 2005 | 20.3 | 15.9 | 24.6 | 19.1 | 22 | 21 |
| | mean | 19.8 | 15.9 | 24.5 | 19.0 | 24 | 20 |
| Observed | 2000 | 13.2 | 16.2 | 16.3 | 19.1 | 23 | 18 |
| | 2002 | 13.0 | 14.4 | 13.6 | 17.9 | 5 | 24 |
| | 2003 | 12.8 | 15.5 | 14.9 | 17.4 | 16 | 12 |
| | 2005 | 12.7 | 17.5 | 15.2 | 19.4 | 20 | 11 |
| | mean | 12.9 | 15.9 | 15.0 | 18.5 | 16 | 16 |
| | range | | | | | 7–26 | −3–40 |

**Table 5.** Slopes, intercepts and $R^2$ values for regressions comparing the simulated yields using the model setups described in Table 3, against reported yields for the 65 NUTS2 level regions. RMSE values and Willmott index ($W_\mathrm{i}$) are provided, the number of data points used to derive the statistics "all" were 1400 (all regions and years).

| Setting | slope | regression intercept | $R^2$ | RMSE | $W_\mathrm{i}$ |
|---|---|---|---|---|---|
| $F_{\mathrm{opt(T,A)}}$, mean | 0.937 | 0.130 | 0.942 | 0.370 | 0.807 |
| $F_{\mathrm{opt(t,A)}}$, mean | 0.820 | 0.805 | 0.801 | 0.588 | 0.721 |
| $F_{\mathrm{opt(T,a)}}$, mean | 0.361 | 4.249 | 0.306 | 0.780 | 0.602 |
| $F_{\mathrm{t,a}}$, mean | 0.228 | 4.510 | 0.082 | 1.243 | 0.353 |
| $F_{\mathrm{t,I}}$, mean | 0.415 | 4.461 | 0.130 | 1.230 | 0.422 |
| $F_{\mathrm{C}}$, mean | −0.209 | 9.516 | 0.075 | 1.845 | 0.074 |
| max($F_{\mathrm{opt(T,A)}}$), mean | 0.247 | 7.453 | 0.051 | 2.627 | −0.343 |
| $F_{\mathrm{opt(T,A)}}$, all | 0.412 | 3.737 | 0.163 | 1.598 | 0.448 |
| $F_{\mathrm{t,I}}$, all | 0.185 | 6.128 | 0.022 | 2.199 | 0.269 |

**Table A1.** The parameters for the factors $f_1$, $f_2$ and $f_3$ (Eqs. 3–5) for spring and winter wheat.

| parameter | | spring | winter |
|---|---|---|---|
| $f_1$: | a | 0.62 | 0.53 |
| | b | −0.02 | 0 |
| | c | 5.8 | 7.63 |
| | d | 0.55 | 0.55 |
| $f_2$: | a | 0.86 | 0.8 |
| | b | 0.19 | 0.2 |
| | c | 28.65 | 13.99 |
| | d | 0.55 | 0.55 |
| $f_3$: | a | 0 | 0 |
| | b | 1 | 1 |
| | c | 8.27 | 8.32 |
| | d | 1.1 | 1.15 |

**Table A2.** A list of variables (in italics) and parameters used in the article with a short description and units.

| variable | description | value | unit | reference |
|---|---|---|---|---|
| LAI | leaf area per ground area | | $m^2\,m^{-2}$ | |
| $M_{s,j}$ | Mass of element $s$ (C, N) in organ $j$ | | $kg\,s\,m^{-2}$ | |
| $m_{s,j}$ | Transport of element $s$ (C, N) in organ $j$ | | $kg\,s\,m^{-2}\,day^{-1}$ | |
| $C:N_j$ | Carbon to nitrogen ratio of organ $j$ | | $kg\,C\,kg^{-1}\,N^{-1}$ | |
| parameter | | | | |
| $C:N_{min,L}$ | Minimum C : N of the leaf | 7 | $kg\,C\,kg^{-1}\,N^{-1}$ | Penning de Vries et al. (1989) |
| $C:N_{max,L}$ | Maximum C : N of the leaf | 35 | $kg\,C\,kg^{-1}\,N^{-1}$ | |
| SLA | Specific leaf area | 45 | $m^2\,kg^{-1}\,C^{-1}$ | Penning de Vries et al. (1989) |
| $d_{r,veg}$ | development rate, vegetative phase | 0.03 | $day^{-1}$ | Wang and Engel (1998) |
| $d_{r,rep}$ | development rate, reproductive phase | 0.042 | $day^{-1}$ | Wang and Engel (1998) |
| $N_b$ | Minimum leaf N content | 0.0011 | $kg\,N\,m^{-2}$ | |
| $\beta_0$ & $\beta_1$ | Regression coefficients $k_L \sim k_N$ | 0.01, 0.52 | | Yin et al. (2003) |

**Table A3.** Nitrogen fertiliser applications and timing for each NUTS2 (Nomenclature of Territorial Units for Statistics in the EU; statistical administrative areas) region used in the regional simulations resulting from optimising modelled yields against observations ($F_{\mathrm{opt(T,A)}}$), see Sect. 3.3, together with the statistics (the 2 last columns). Number of years with reported yields for each region (n. y), fraction of the wheat area covered by winter variety (Ar.), fraction with spring variety: 1 – Ar., reported yields and AgGrid N input data for each region.

| | | | Winter wheat | | | Spring wheat | | | AgGrid | | | | | |
|---|---|---|---|---|---|---|---|---|---|---|---|---|---|---|
| | | | N Timing, DS | | | N Timing, DS | | | input | | Yields | | Statistics | |
| NUTS2 | n. y | Ar. | 0 | 0.5 | kg N ha$^{-1}$ | 0 | 0.5 | kg N ha$^{-1}$ | kg N ha$^{-1}$ | Mod. | Rep. | RMSE | Willm. |
| BE10 | 25 | 0.97 | 0.00 | 0.00 | 100 | 0.00 | 1.00 | 50 | 282 | 6.41 | 6.52 | 2.34 | 0.48 |
| BE21 | 31 | 0.81 | 0.00 | 0.00 | 250 | 0.00 | 1.00 | 50 | 257 | 5.50 | 5.73 | 1.30 | 0.45 |
| BE22 | 31 | 0.95 | 0.33 | 0.33 | 250 | 0.00 | 1.00 | 50 | 271 | 7.21 | 7.43 | 1.94 | 0.36 |
| BE23 | 31 | 0.91 | 0.00 | 0.00 | 150 | 0.00 | 1.00 | 50 | 263 | 6.79 | 6.98 | 1.63 | 0.46 |
| BE24 | 19 | 0.97 | 0.00 | 0.00 | 200 | 0.00 | 1.00 | 50 | 282 | 7.72 | 7.84 | 1.45 | 0.05 |
| BE25 | 31 | 0.97 | 0.33 | 0.00 | 250 | 0.00 | 0.00 | 250 | 139 | 6.64 | 7.49 | 2.14 | 0.23 |
| BE31 | 19 | 0.97 | 0.67 | 0.00 | 150 | 0.33 | 0.00 | 200 | 282 | 7.90 | 8.26 | 1.44 | −0.15 |
| BE32 | 31 | 0.98 | 0.00 | 0.00 | 150 | 0.33 | 0.67 | 50 | 163 | 7.06 | 7.29 | 1.56 | 0.35 |
| BE33 | 31 | 0.96 | 0.33 | 0.00 | 250 | 0.00 | 1.00 | 100 | 263 | 7.52 | 7.77 | 1.71 | 0.34 |
| BE34 | 31 | 0.98 | 0.00 | 0.00 | 100 | 0.00 | 1.00 | 150 | 178 | 4.92 | 5.11 | 1.11 | 0.36 |
| BE35 | 31 | 0.97 | 0.00 | 0.00 | 150 | 0.00 | 1.00 | 50 | 177 | 6.89 | 6.91 | 1.40 | 0.47 |
| DE26 | 7 | 0.98 | 0.33 | 0.33 | 150 | 0.00 | 0.00 | 200 | 185 | 5.31 | 5.85 | 1.07 | −0.16 |
| DE41 | 3 | 0.96 | 0.00 | 0.00 | 250 | 0.33 | 0.00 | 250 | 166 | 5.60 | 5.63 | 1.17 | 0.55 |
| DE50 | 7 | 0.97 | 0.00 | 0.00 | 100 | 0.33 | 0.00 | 250 | 185 | 5.23 | 5.88 | 1.57 | 0.35 |
| DE60 | 19 | 0.98 | 0.00 | 1.00 | 200 | 0.67 | 0.00 | 50 | 185 | 6.54 | 6.94 | 1.92 | −0.03 |
| DE71 | 6 | 0.98 | 0.00 | 0.33 | 250 | 0.00 | 0.00 | 150 | 185 | 6.00 | 6.46 | 1.54 | 0.02 |
| DE72 | 6 | 0.97 | 0.00 | 0.33 | 250 | 0.00 | 0.00 | 150 | 185 | 6.02 | 6.50 | 1.58 | −0.03 |
| DE73 | 6 | 0.97 | 0.00 | 0.33 | 250 | 0.00 | 1.00 | 50 | 185 | 6.49 | 6.68 | 1.50 | 0.07 |
| DE80 | 15 | 0.97 | 0.00 | 0.00 | 200 | 0.00 | 0.00 | 250 | 183 | 6.25 | 6.73 | 1.23 | 0.25 |
| DE91 | 7 | 0.98 | 0.00 | 0.67 | 200 | 0.00 | 0.67 | 100 | 185 | 6.69 | 7.18 | 1.79 | 0.22 |
| DE92 | 7 | 0.98 | 0.00 | 0.00 | 200 | 0.00 | 0.00 | 200 | 185 | 6.70 | 7.29 | 2.13 | 0.12 |
| DE93 | 7 | 0.97 | 0.00 | 1.00 | 150 | 0.00 | 1.00 | 50 | 185 | 6.26 | 6.55 | 1.76 | 0.18 |
| DE94 | 7 | 0.96 | 0.00 | 0.00 | 100 | 0.00 | 0.00 | 200 | 211 | 6.00 | 6.64 | 1.67 | 0.30 |
| DEA1 | 7 | 0.97 | 0.00 | 0.00 | 150 | 0.00 | 1.00 | 50 | 232 | 6.99 | 7.22 | 1.70 | 0.31 |
| DEA2 | 7 | 0.97 | 0.00 | 1.00 | 150 | 0.00 | 1.00 | 50 | 208 | 7.67 | 7.59 | 1.57 | 0.36 |
| DEA3 | 7 | 0.97 | 0.00 | 1.00 | 150 | 0.00 | 0.00 | 100 | 203 | 6.38 | 6.91 | 1.92 | 0.26 |
| DEA4 | 7 | 0.98 | 0.33 | 0.67 | 150 | 0.00 | 0.67 | 150 | 185 | 6.38 | 6.99 | 2.23 | 0.18 |
| DEA5 | 7 | 0.98 | 0.00 | 1.00 | 150 | 1.00 | 0.00 | 50 | 185 | 6.79 | 7.06 | 2.09 | 0.28 |
| DEB1 | 7 | 0.98 | 0.00 | 0.33 | 100 | 1.00 | 0.00 | 50 | 185 | 5.52 | 5.78 | 1.23 | 0.15 |
| DEB2 | 7 | 0.97 | 0.33 | 0.33 | 50 | 0.00 | 1.00 | 150 | 185 | 4.95 | 5.31 | 1.19 | 0.34 |
| DEB3 | 7 | 0.98 | 0.00 | 0.33 | 200 | 0.00 | 1.00 | 50 | 185 | 5.69 | 5.68 | 1.06 | 0.23 |
| DEC0 | 26 | 0.99 | 0.00 | 0.00 | 100 | 0.00 | 1.00 | 50 | 183 | 5.37 | 5.44 | 1.04 | 0.45 |
| DEE3 | 2 | 0.98 | 0.33 | 0.67 | 250 | 0.00 | 0.33 | 250 | 185 | 6.97 | 7.84 | 0.90 | −0.01 |
| DEF0 | 26 | 0.97 | 0.00 | 1.00 | 250 | 0.00 | 1.00 | 50 | 184 | 7.81 | 7.87 | 2.00 | −0.07 |

**Table A3.** Continued.

| | | | Winter wheat | | | Spring wheat | | AgGrid | | Yields | | Statistics | |
|---|---|---|---|---|---|---|---|---|---|---|---|---|---|
| | | | N Timing, DS | | | N Timing, DS | | input | | | | | |
| NUTS2 | n. y | Ar. | 0 | 0.5 | kg N ha$^{-1}$ | 0 | 0.5 | kg N ha$^{-1}$ | kg N ha$^{-1}$ | Mod. | Rep. | RMSE | Willm. |
| FR10 | 28 | 1.00 | 0.00 | 0.00 | 200 | 0.00 | 1.00 | 50 | 110 | 7.15 | 7.29 | 1.41 | 0.21 |
| FR21 | 29 | 1.00 | 0.00 | 0.00 | 200 | 0.00 | 1.00 | 50 | 110 | 7.41 | 7.35 | 1.29 | 0.28 |
| FR22 | 29 | 1.00 | 0.00 | 0.00 | 200 | 0.33 | 0.67 | 50 | 110 | 7.32 | 7.60 | 1.58 | 0.21 |
| FR23 | 29 | 1.00 | 0.00 | 0.00 | 150 | 0.00 | 0.67 | 50 | 110 | 7.21 | 7.37 | 1.39 | 0.20 |
| FR24 | 29 | 0.99 | 0.00 | 0.00 | 100 | 0.00 | 1.00 | 50 | 110 | 6.20 | 6.32 | 1.14 | 0.34 |
| FR25 | 29 | 1.00 | 0.00 | 0.00 | 200 | 0.33 | 0.00 | 200 | 110 | 6.56 | 6.85 | 1.40 | 0.20 |
| FR26 | 29 | 1.00 | 0.00 | 0.00 | 100 | 0.33 | 0.00 | 250 | 110 | 5.61 | 6.02 | 1.18 | 0.27 |
| FR30 | 28 | 1.00 | 0.00 | 0.00 | 200 | 0.00 | 1.00 | 50 | 110 | 7.39 | 7.62 | 1.87 | 0.13 |
| FR41 | 29 | 1.00 | 0.00 | 0.00 | 200 | 0.00 | 1.00 | 50 | 114 | 5.90 | 6.03 | 1.33 | 0.37 |
| FR51 | 29 | 0.99 | 0.00 | 0.00 | 100 | 0.00 | 0.00 | 200 | 110 | 5.53 | 5.84 | 1.35 | 0.30 |
| FR52 | 29 | 0.97 | 0.00 | 0.00 | 100 | 0.00 | 1.00 | 50 | 110 | 6.22 | 6.22 | 1.22 | 0.38 |
| FR53 | 29 | 0.99 | 0.00 | 0.00 | 100 | 0.00 | 0.00 | 250 | 110 | 5.31 | 5.63 | 1.19 | 0.27 |
| FR61 | 29 | 0.96 | 0.00 | 0.67 | 100 | 0.00 | 1.00 | 50 | 110 | 4.94 | 4.96 | 1.38 | 0.14 |
| FR63 | 29 | 1.00 | 0.00 | 0.67 | 50 | 0.00 | 1.00 | 50 | 110 | 4.46 | 4.47 | 0.95 | 0.44 |
| FR72 | 29 | 1.00 | 0.33 | 0.00 | 100 | 0.33 | 0.00 | 250 | 110 | 5.20 | 5.51 | 1.11 | 0.32 |
| LU00 | 28 | 0.96 | 0.33 | 0.00 | 50 | 0.00 | 1.00 | 150 | 162 | 4.98 | 5.24 | 1.12 | 0.39 |
| NL11 | 31 | 0.85 | 0.00 | 0.00 | 150 | 0.00 | 0.00 | 250 | 257 | 7.22 | 7.45 | 1.70 | 0.13 |
| NL12 | 31 | 0.84 | 0.33 | 0.00 | 250 | 0.00 | 0.00 | 200 | 257 | 7.28 | 7.58 | 1.85 | 0.00 |
| NL13 | 31 | 0.87 | 0.00 | 0.00 | 100 | 0.00 | 1.00 | 50 | 257 | 6.18 | 6.32 | 1.18 | 0.18 |
| NL21 | 30 | 0.91 | 0.00 | 0.00 | 200 | 1.00 | 0.00 | 150 | 257 | 6.27 | 6.49 | 1.39 | 0.06 |
| NL22 | 30 | 0.91 | 0.33 | 0.00 | 250 | 0.00 | 0.00 | 200 | 257 | 7.15 | 7.50 | 2.06 | 0.10 |
| NL23 | 30 | 0.85 | 0.67 | 0.00 | 250 | 0.00 | 0.00 | 250 | 257 | 7.29 | 8.17 | 2.39 | −0.20 |
| NL31 | 31 | 0.82 | 0.00 | 0.00 | 100 | 0.00 | 1.00 | 50 | 257 | 5.96 | 6.27 | 2.21 | 0.43 |
| NL32 | 31 | 0.82 | 0.00 | 0.00 | 250 | 0.00 | 0.67 | 50 | 257 | 7.37 | 7.93 | 1.83 | −0.16 |
| NL33 | 31 | 0.83 | 0.00 | 0.00 | 250 | 0.00 | 0.00 | 200 | 257 | 7.63 | 8.21 | 1.93 | −0.20 |
| NL34 | 31 | 0.86 | 0.00 | 0.00 | 250 | 0.00 | 0.00 | 200 | 257 | 7.96 | 8.31 | 1.76 | −0.01 |
| NL41 | 31 | 0.86 | 0.33 | 0.33 | 250 | 0.00 | 0.00 | 200 | 257 | 7.39 | 7.89 | 2.01 | −0.21 |
| NL42 | 31 | 0.94 | 0.00 | 0.00 | 200 | 0.00 | 0.00 | 200 | 257 | 6.81 | 7.31 | 1.54 | 0.12 |
| UKH | 12 | 0.82 | 0.00 | 0.00 | 150 | 1.00 | 0.00 | 250 | 148 | 8.04 | 8.07 | 1.31 | −0.46 |
| UKJ | 11 | 0.82 | 0.00 | 0.00 | 200 | 0.00 | 0.00 | 250 | 148 | 7.65 | 7.75 | 1.10 | −0.31 |
| UKK | 29 | 0.81 | 0.00 | 0.00 | 150 | 0.00 | 1.00 | 150 | 148 | 6.62 | 6.71 | 1.32 | 0.10 |

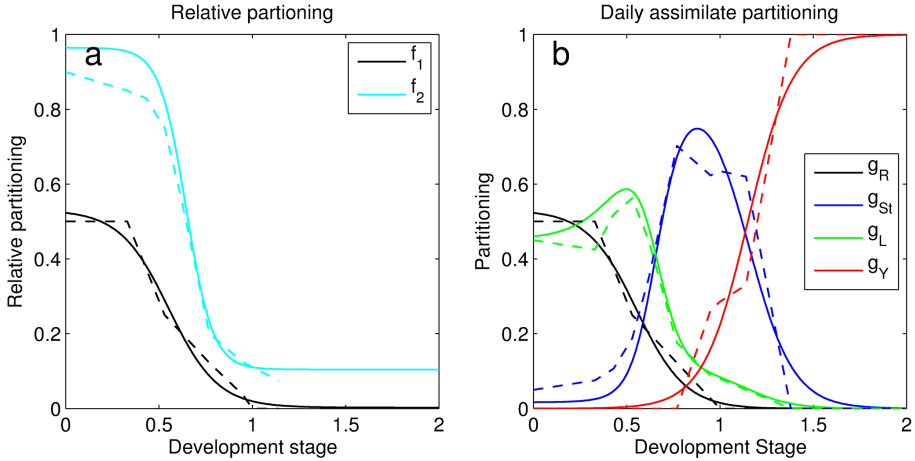


**Figure 1. (a)** The allocation to roots relative to vegetative organs ($f_1$) and the allocation to leaves relative to leaves and stem ($f_2$) for winter wheat. Dashed lines represent the allocation model from Penning de Vries et al. (1989) and solid lines are fitted Richards equations (Eqs. 3 and 4). **(b)** The resulting allocation scheme to roots ($g_R$), stem ($g_{St}$), leaves ($g_L$) and grains ($g_Y$) (solid lines) compared to data from Penning de Vries et al. (1989) (dashed lines) from equations in Eq. (6).

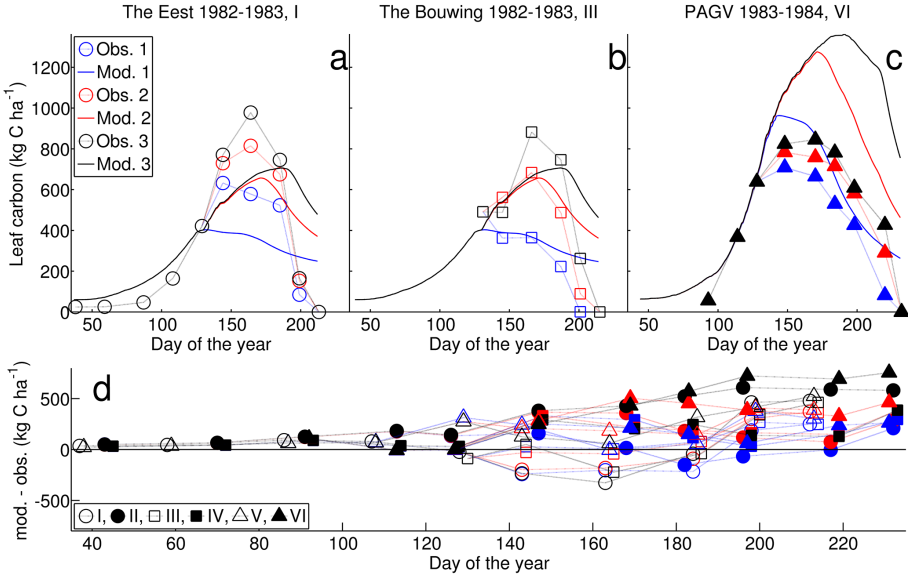


**Figure 2. (a–c)** Observed (thin lines) and simulated (thick lines) leaf C for the Eest and Bouwing for the season 1982–1983 and PAGV for the season 1983–1984, for three example plots with different levels of N fertiliser input. **(d)** The difference between observed and simulated leaf C for three different levels of fertiliser application for the Bouwing, the Eest and PAGV (Netherlands) for seasons 1982–1983 and 1983–1984 (Groot and Verberne, 1991). Blue symbols indicate lowest levels of fertilisation; red represent medium and black symbols a high N fertiliser input. Open symbols are for the season 1982–83, and closed symbols are for the season 1983–1984.

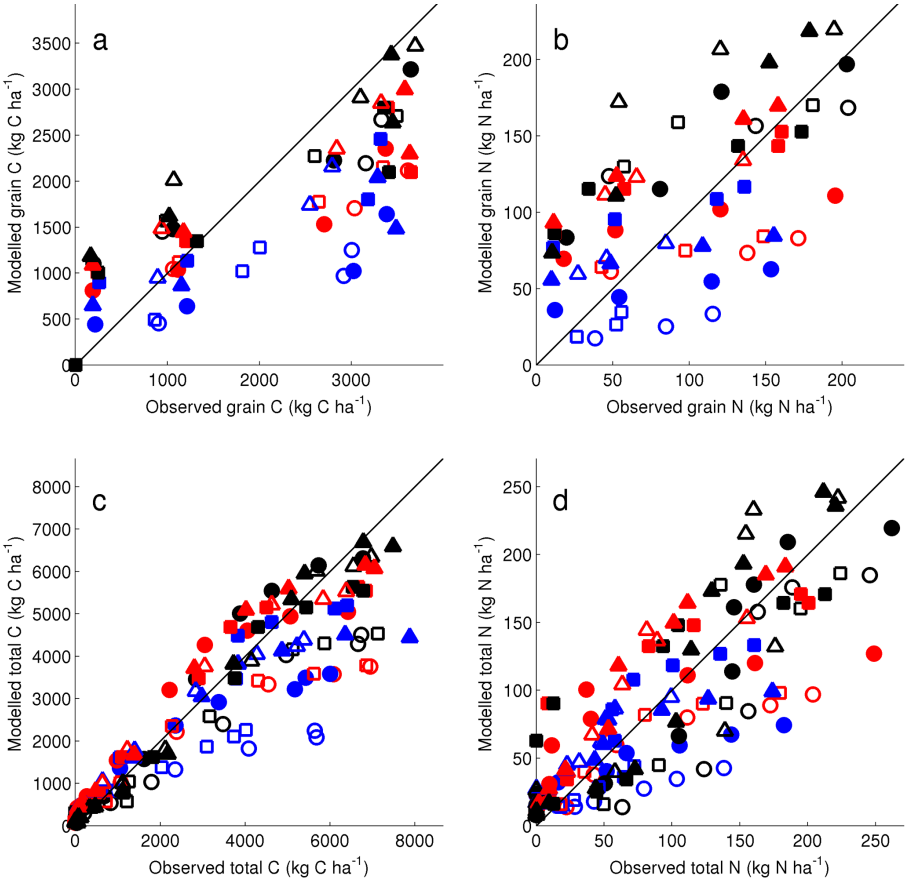


**Figure 3.** A comparison between modelled and observed grain C **(a)** and N **(b)**, and total biomass C **(c)** and N **(d)** for the Eest, the Bouwing and PAGV, the Netherlands over the growing-seasons 1982–1983 and 1983–1984. Symbols the same as in Fig. 2 with blue symbols for low input of N fertiliser, red for a medium input of N and black for high N input.

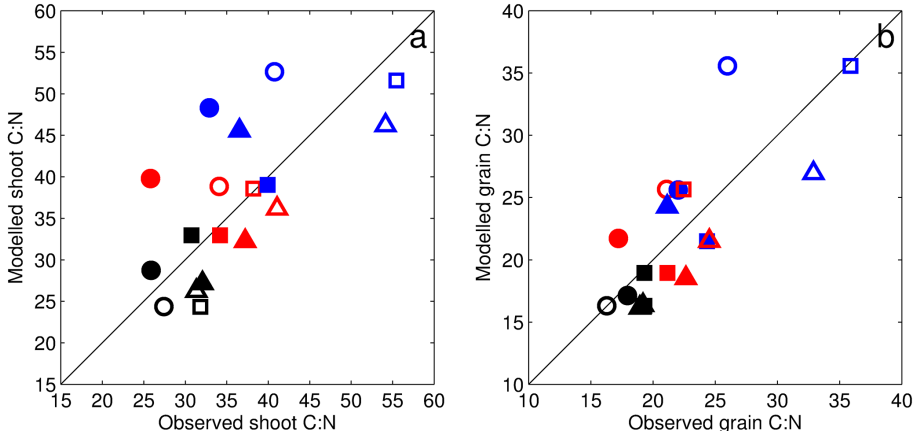


**Figure 4.** A comparison between modelled and observed C : N in harvested above-ground biomass **(a)** and grains **(b)**, for the Eest, the Bouwing and PAGV, the Netherlands for the seasons 1982–1983 and 1983–1984. Symbols the same as in Fig. 2 with blue symbols for low input of N fertiliser, red for a medium input of N and black for high N input.

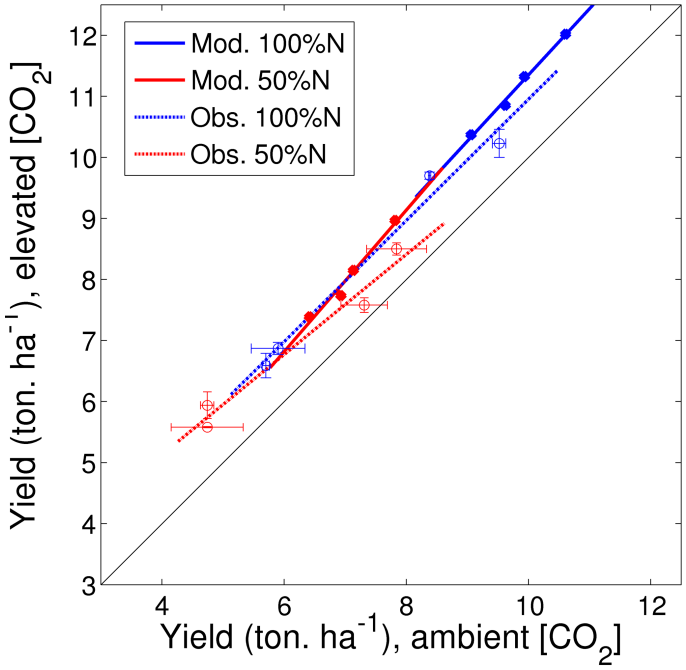


**Figure 5.** Effect of $CO_2$ fertilisation on observed and simulated grain yield, comparing wheat grain yields grown at elevated $CO_2$ ($\sim$ 548 ppm) with those grown at ambient $CO_2$ ($\sim$ 378 ppm). Simulated yields are depicted by solid lines and filled circles, observations are depicted by dashed lines and markers, shown for treatments with sufficient N fertiliser input (100 % N, blue), and treatments that received half of that amount (50 % N, red). Observations are from (Table 4 Weigel and Manderscheid, 2012).

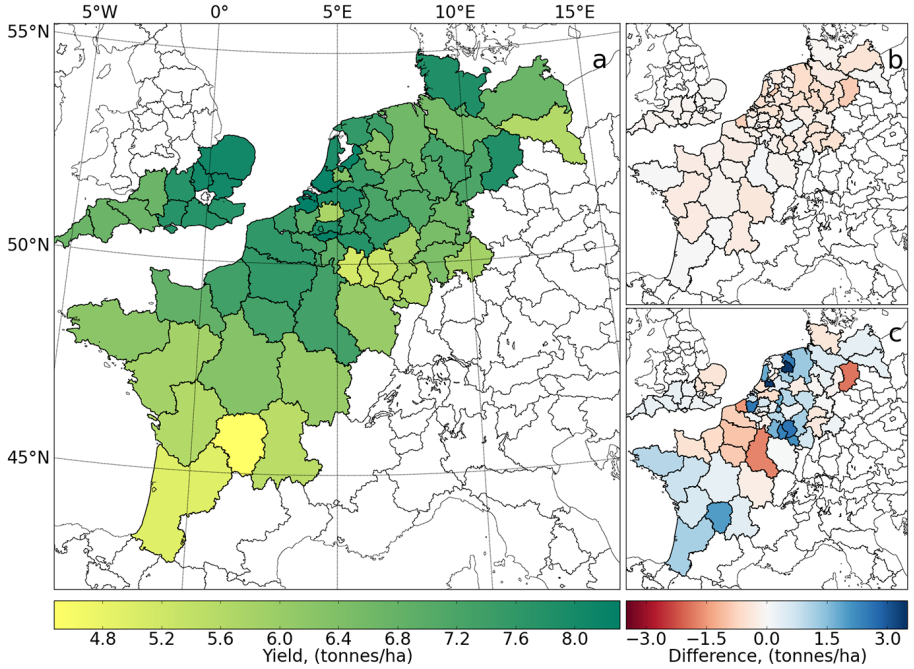


**Figure 6.** Reported regional yields from EUROSTAT **(a)**, differences between simulated and reported yields for the $F_{\mathrm{opt(T,A)}}$ setup **(b)** and the $F_{\mathrm{t,I}}$ **(c)** simulations.

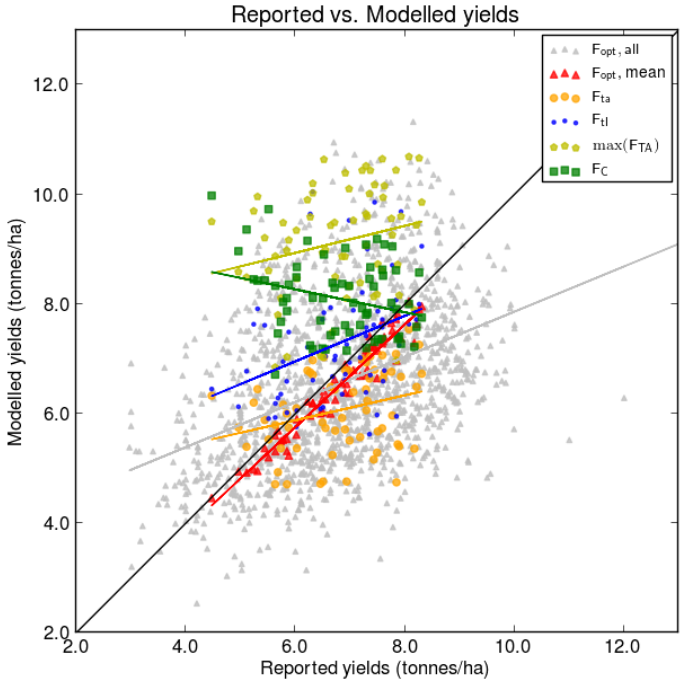


**Figure 7.** Reported vs. modelled yields for the 65 regions used in this study. Grey triangles represent all available years for each region, with the fertiliser management that gave the best agreement with data for each region ($F_{\text{opt(T,A)}}$, all), the red markers are their means. Dark green markers show the mean for each region with the C-only version of the model ($F_{\text{C}}$), pale green represent the management that gave the maximum yields for each region (max($F_{\text{T,A}}$)). Orange markers show the result from using a mean N management over the region, blue represent simulations using the same timing for each region but with a spatially explicit data set of N application (Elliott et al., 2014) ($F_{\text{t,l}}$). Lines are fitted linear regressions, see Table 5 for details. The number of years included for each region is listed in Table A3.

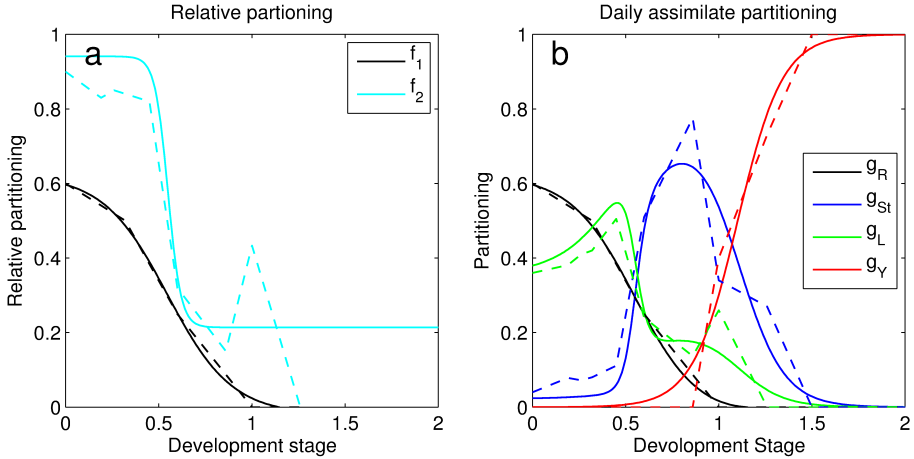


**Figure A1. (a)** Tthe allocation to roots relative that to vegetative organs ($f_1$) and the allocation to leaves relative that to leaves and stem ($f_2$) for spring wheat. Dashed lines represent the allocation model from Penning de Vries et al. (1989) and solid lines are fitted Richards equations (Eqs. 3 and 4). **(b)** The resulting allocation scheme to roots ($g_{\mathrm{R}}$), stem ($g_{\mathrm{St}}$), leaves ($g_{\mathrm{L}}$) and grains ($g_{\mathrm{Y}}$) (solid lines) compared to data from Penning de Vries et al. (1989) (dashed lines) from equations in Eq. (6).

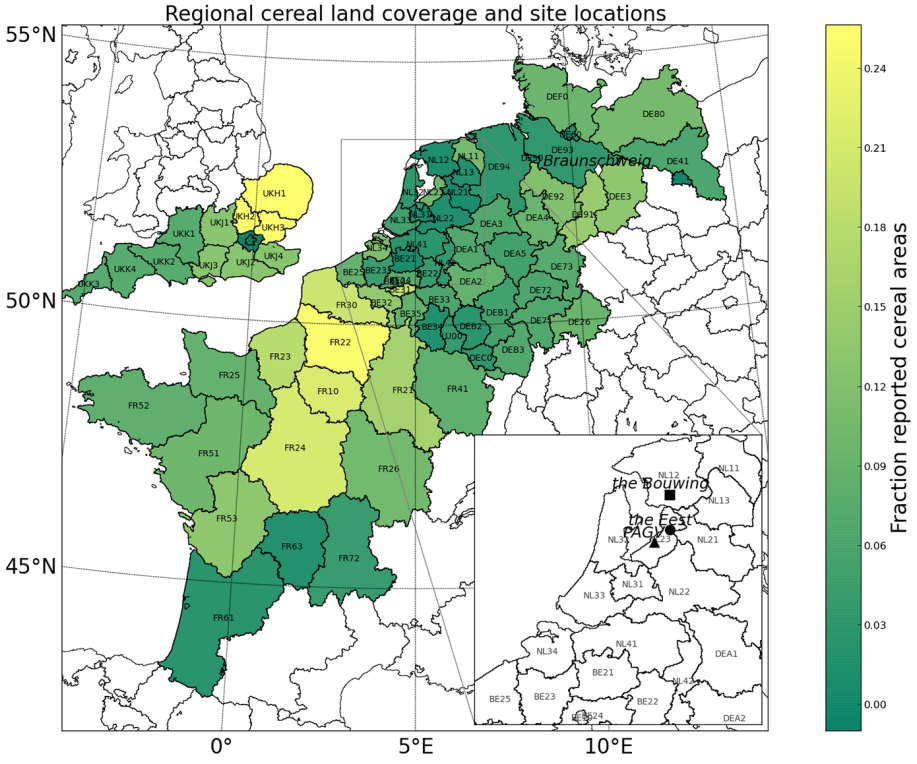


**Figure A2.** The fractions of cereal land in each selected region from EUROSTAT with region names as labels, also the locations of the trials described in Sect. 3.1 and the FACE experimental site.

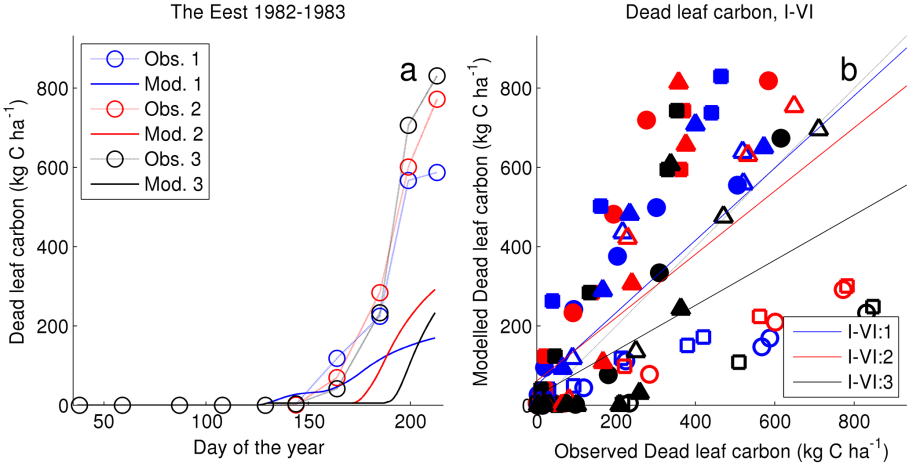


**Figure A3. (a)** Dead leaf comparison between modelled (thick lines) and observations for the Eest, the Netherlands 1982–1983. Blue lines; are with 0 input of N fertiliser, red lines; with an input of 60 kg N ha$^{-1}$ and black lines; 160 kg N ha$^{-1}$. **(b)** A comparison between modelled and observed C mass of dead leaves for winter wheat for the Eest (○), the Bouwing (□) and PAGV (△), the Netherlands for the seasons 1982–1983 and 1983–1984. Blue symbols; are with a low input of N fertiliser, red; with a medium input of N and black; a high input. Open symbols are for the season 1982–83, and closed symbols are for the season 1983–1984.